

1
2 **A tale of winglets: evolution of flight morphology in stick insects**
3

4 Yu Zeng^{1,2,†}, Conner O’Malley¹, Sonal Singhal^{1,3}, Faszly Rahim^{4,5},
5 Sehoon Park¹, Xin Chen^{6,7}, Robert Dudley^{1,8}

6
7 ¹Department of Integrative Biology, University of California, Berkeley, CA 92870,
8 USA

9 ²Schmid College of Science and Technology, Chapman University, Orange, CA
10 92866, USA

11 ³ Department of Biology, CSU Dominguez Hills, Carson, CA 90747 USA

12 ⁴Islamic Science Institute (ISI), Universiti Sains Islam Malaysia, 71800 Bandar Baru
13 Nilai, Negeri Sembilan, Malaysia

14 ⁵Centre for Insect Systematics (CIS), Universiti Kebangsaan Malaysia, 43600
15 Bangi, Selangor, Malaysia

16 ⁶Department of Biology, The College of Staten Island, The City University of New
17 York, NY 10314, USA

18 ⁷Department of Biology, The Graduate School and University Center, The City
19 University of New York, NY 10016, USA

20 ⁸Smithsonian Tropical Research Institute, Balboa,
21 Republic of Panama

22
23 [†]Corresponding author: dreavoniz@berkeley.edu

26

Abstract

27

The evolutionary transition between winglessness and a full-winged morphology requires selective advantage for intermediate forms. Conversely, repeated secondary wing reductions among the pterygotes indicates relaxation of such selection. However, evolutionary trajectories of such transitions are not well characterized. The stick insects (Phasmatodea) exhibit diverse wing sizes at both interspecific and intersexual levels, and thus provide a system for examining how selection on flight capability, along with other selective forces, drives the evolution of flight-related morphology. Here, we examine variation in relevant morphology for stick insects using data from 1100+ individuals representing 765 species. Although wing size varies along a continuous spectrum, taxa with either long or miniaturized wings are the most common, whereas those with intermediate-sized wings are relatively rare. In a morphological space defined by wing and body size, the aerodynamically relevant parameter termed wing loading (the average pressure exerted on the air by the wings) varies according to sex-specific scaling laws; volant but also flightless forms are the most common outcomes in both sexes. Using phylogenetically-informed analyses, we show that wing size and body size are correlated in long-wing insects regardless of sexual differences in morphology and ecology. These results demonstrate the diversity of flight-related morphology in stick insects, and also provided a general framework for addressing evolutionary coupling between wing and body size. We also find indirect evidence for a ‘fitness valley’ associated with intermediate-sized wings, suggesting relatively rapid evolutionary transitions between wingless and volant forms.

49

50

51

Keywords

52

body size, evolution, flight, phasmid, sexual dimorphism, wing size

53

54

55

56

57

Symbols and abbreviations

58

A_w	Wing area
p_w	Wing loading
L	Body length
L_w	Wing length
m	Mass
SSD	Sexual size dimorphism
SWD	Sexual wing dimorphism
Q	Relative wing size
ΔL	Sexual size dimorphism index
ΔQ	Sexual wing dimorphism index

59

60

61

62

63

64

65

66

67

68

69

70

71

72 **1. Introduction**

73
74 Flight is fundamental to the ecology and evolutionary diversification of pterygote insects by
75 allowing for three-dimensional mobility and greater access to nutritional resources (Dudley,
76 2000). Nonetheless, approximately 5% of the extant pterygote fauna is flightless (Roff, 1994),
77 and various conditions of reduced wing size (e.g., brachyptery and microptery) are found across
78 the neopteran orders. Given structural costs and high energy expenditure during flight,
79 maintenance of the flight apparatus is not universally favored by selection. Partial reduction or
80 complete loss of wings is associated with various morphological and ecological factors, such as
81 developmental tradeoffs, enhanced female fecundity, and reduced demand for aerial mobility in
82 certain habitats (Roff, 1990; Roff, 1994). In these cases, smaller wings exhibit reduced
83 aerodynamic capability, but may serve secondarily derived non-aerodynamic functions such as
84 use in protection, stridulation, and startle displays (see Dudley, 2000).

85
86 Wing evolution can also be influenced indirectly by selection on overall body
87 size. Generally, reduced body mass enables greater maneuverability in flight (e.g., more rapid
88 translational and rotational accelerations), although numerous factors influence insect size
89 evolution (see Blanckenhorn, 2000; Chown and Gaston, 2010). Furthermore, both flight
90 capacity and body size can be subject to sex-specific selection. As a consequence, sexual size
91 dimorphism (SSD) is typically associated with intersexual niche divergence and with sexual
92 selection (see Shine, 1989; Hedrick and Temeles, 1989). Sexual wing dimorphism (SWD) can in
93 some cases be decoupled from SSD, and may be associated with divergence in aerial niche and
94 wing use (e.g., DeVries et al., 2010). Selection for greater locomotor capacity in males can lead
95 to male-biased SWD, and also to female-biased SSD (see Roff, 1986). It is therefore of interest
96 to consider patterns of sexual dimorphism in both wing and body size within a phylogenetic
97 context.

98
99 The stick insects (Phasmatodea) exhibit great diversity in both wing and body size (**Fig. 1,**
100 **2**), but underlying evolutionary patterns are not well characterized. Most winged stick insects
101 possess rudimentary and tegmenized forewings. Phasmid hindwings (designated ‘wings’
102 hereafter) can be of various sizes and exhibit expanded cubital and anal venation with well-
103 developed flight membranes. Fossil evidence suggest that both wing pairs were full-sized in
104 ancestral stick insects (see Shang et al., 2011; Wang et al., 2014), whereas numerous extant
105 species exhibit wing reduction. Earlier studies have proposed frequent evolutionary transitions
106 between winged and wingless morphologies, although the directionality and the detailed
107 dynamics of phasmid wing evolution remain contested (see Whiting et. al., 2003; Stone and
108 French, 2003; Trueman et al., 2004; Whiting and Whiting, 2004; Goldberg and Igić, 2008).
109 Nevertheless, size-reduced wings must lead to degradation in aerodynamic performance, with
110 possibly concurrent changes in body length and mass. Given the unresolved history of wing size
111 evolution of this group, we use the term ‘reduction’ to describe wings that are developmentally
112 truncated relative to a full-sized morphology, without assessing the directionality of wing size
113 evolution within the group’s phylogeny.

114
115 Here, we examine the evolution of phasmid flight morphology on a macroevolutionary
116 scale. We first describe variation in wing and body size using data from 1100+ individuals across
117 765 species, including intraspecific data from the *Ascales tanarata* species group with three

118 subspecies exhibiting altitudinal variation in both wing and body size (see Brock, 1999; Seow-
119 Choen and Brock, 1999; **Fig. 2b**). This group represents one of the few well-documented cases
120 of features of flight morphology being distinctly correlated with a gradient in environmental
121 parameters. We also assess the allometry of wing loading, and use phylogenetic correlational
122 analyses to assess the evolutionary interaction between changes in wing size (reflecting flight
123 ability) and overall body size. Sexual differences in flight-related morphology (e.g., wing
124 allometry) and ecology (e.g., greater demand for mate search by males) may derive from sex-
125 specific interactions between selective forces, and we thus also examine correlations between
126 SWD and SSD. For example, if selection on male-biased mobility and on female-biased
127 fecundity were coupled, we might expect an inverse correlation between SWD and SSD. We
128 accordingly assess overall patterns of sexual dimorphism among phasmid species within
129 phylogenetic and allometric contexts.

130
131

132 **2. Materials and Methods**

133 **Morphometrics**

134 Our sampling primarily focused on winged phasmid clades, given available data (see
135 **Supplementary Fig. S1**). Wing length (L_w) and body length (L) data were primarily obtained
136 from literature sources, and were enriched with measurements on both captive-reared and field-
137 collected insects (see section ‘Scaling of wing loading’). Taxonomic justification followed
138 Phasmida Species File (Brock, 2019), downloaded and formatted using custom-written scripts in
139 MatLab (Supplementary Materials). For the *A. tanarata* species group, male and females of three
140 subspecies were collected in the field (see also Brock, 1999). The main dataset includes
141 measurements on 599 males and 533 females from 765 species (~23% of 3348 known species),
142 of which 367 species included data on both sexes (**Supplementary Dataset 1**). If available,
143 mean measurements were used; otherwise, median values were calculated based on ranges
144 between maximum and minimum values. The relative wing size (Q) was defined as the ratio of
145 wing length to body length:

$$147 \quad Q = L_w/L \quad (1)$$

146

148 SWD was measured by the SWD index (ΔQ), calculated as:

$$149 \quad \Delta Q = (L_{w,M} - L_{w,F})/(L_{w,M} + L_{w,F}) \quad (2)$$

150

151 where the subscripts M and F denote male and female, respectively. The sign and magnitude of
152 ΔQ thus represent the type and level of SWD. For example, $\Delta Q < 0$ represents female-biased
153 SWD, $\Delta Q = 0$ represents a lack of SWD, and $\Delta Q = 1$ when the female is wingless and the male
154 is winged. Similarly, SSD was measured by the SSD index (ΔL), which was calculated as:

$$155 \quad \Delta L = (L_M - L_F)/(L_M + L_F) \quad (3)$$

156

157

158 **Scaling of wing loading**

159 The loss of aerodynamic capability was assessed using wing loading, the ratio of body weight to
160 total wing area. We sampled total wing area (A_w), body mass (m) and L from 23 males and 21
161 females of field-collected and captive-bred insects from 36 species (**Supplementary Dataset 2**).
162 Digital images were obtained dorsally for insects placed on horizontal surfaces with all legs
163 laterally extended; projected areas of fully unfolded wings were manually extracted using
164 Photoshop (CS6, Adobe Systems Inc., San Jose, CA, USA). A_w , L_w and L were measured using
165 ImageJ (Schneider et al., 2012). The scaling of wing loading (p_w) with Q was analyzed for both
166 sexes. First, we examined the allometric scaling of body mass based on the formula:

$$167 \quad m = C_1 L^a \quad (4)$$

168

169 where C_1 is the slope coefficient. Similarly, the power-law scaling of A_w with Q can be
170 expressed as:

171
$$A_w = C_2 L_w^b = C_2 (LQ)^b \quad (5)$$

172

173 Combining Eqn. 4 and 5, we have:

175
$$p_w = \frac{mg}{A_w} = C_1 C_2 L^{a-b} Q^{-b} \quad (6)$$

174

176 For a given L, Eqn. 6 was further simplified as:

177
$$p_w = C Q^{-b} \quad (7)$$

178

179 where the slope coefficient $C = C_1 C_2 L^{a-b}$.

180

181 Bayesian phylogenetic reconstruction

182 We used three mitochondrial genes (cytochrome oxidase subunit I (COI) gene, cytochrome
183 oxidase subunit II (COII) gene, and large subunit rRNA (28S) gene; total length 2149 bp) and
184 one nuclear gene (histone subunit 3 (H3) gene; 350 bp) (primer details in **Supplementary Table**
185 **S1**). Our molecular sequencing covered nine species, including all three taxa from the *A.*
186 *tanarata* group (**Supplementary Dataset 3**). We extracted total genomic DNA from leg tissue
187 using a modified high-salt protocol (Aljanabi and Martinez, 1997) and, subsequently, quantified
188 and diluted the DNA using a Nanodrop spectrometer. We amplified each loci using standard
189 PCR conditions. Amplified products were cleaned with Exosap and sequenced using PCR
190 primers with BigDye v3.1 on an Applied Biosystems 3730 machine. For other species, we
191 downloaded sequence data from the same four genes from GenBank. Our molecular data set
192 covers about 70% of the recognized tribes of Phasmatodea (Brock et al., 2019) and two outgroup
193 species (Embioptera), with 95% of the species > 95% complete by locus.

194 Sequences were assembled in Geneious (v6.1.7, Biomatters) and aligned using the
195 MUSCLE algorithm (Edgar, 2004). Gene alignments were checked manually for accuracy.
196 jModelTest v0.1.1 was used to determine the best fitting substitution model for each gene based
197 on the Akaike Information Criterion (AIC) (Posada, 2008). Next, we estimated a time-calibrated
198 phylogeny in BEAST package (v1.10.4; Drummond et al., 2012). Across genes, we used
199 unlinked substitution models and linked clock and tree models. To date the phylogeny, we used
200 the fossil crown group phasmid *Renphasma sinica* dated 122 Myr ago (Nel and Delfosse, 2011)
201 to set the minimum age of the divergence between Embioptera and Phasmatodea. Also, we
202 included two fossil calibrations, following Buckley et al. (2008). Fossil Euphasmatodean eggs
203 from mid-Cretaceous dated to 95–110 Myr ago were used (see Rasnitsyn and Ross, 2000;
204 Grimaldi and Engel, 2005) to determine the age of the most recent ancestor of Euphasmatodea.
205 The sister group relationship between *Timema* and Euphasmatodea has been confirmed by both
206 morphological and molecular evidence (Whiting et al., 2003; Bradler, 2009). Therefore, we
207 assumed the divergence between Euphasmatodea and *Timema* occurred more than 95 Myr ago.
208 Furthermore, we used fossil leaf insect dated 47 Myr ago (Wedmann et al., 2007) and fossil eggs
209 of Anisomorphini dated 44 Myr ago (Sellick, 1994) to set the minimum age of the nodes of the
210 most recent common ancestors of leaf insects and Pseudophasmatinae, respectively. We first
211 optimized the Markov chain Monte Carlo (MCMC) operator by performing short runs (1×10^7
212 cycles) with a relaxed lognormal model and a Yule model, and adjusted the operators as

213 suggested by the program. Then, we ran ten analyses for 2×10^8 generations each. We monitored
214 convergence and determined the burn-in using TRACER v1.7 (Rambaut et al., 2018). After
215 discarding burn-in (25%), we used a maximum credibility approach to infer the consensus tree in
216 TreeAnnotator v1.10.4.

217

218 Phylogenetic correlations

219 A total of five morphological traits was used in phylogenetic analyses (L and Q of both sexes
220 and sex-averaged L, ΔQ , and ΔL). First, we calculated the phylogenetic signals (λ) for all
221 characters using the maximum-likelihood approach implemented in Phytools (Pagel, 1999;
222 Revell, 2012). This model was compared with alternative models where λ was forced to be 1 or 0
223 in order to find the best-fitting model. The best-fitting model was found using the likelihood ratio
224 (LR) test,

$$225 \quad LR = -2 \times (Lh_{\text{better fitting model}} - Lh_{\text{worse fitting model}}) \quad (8)$$

227 whereby the better fitting model has the highest log-likelihood score, Lh (Pagel, 1997, 1999;
228 Freckleton et al., 2002). When $\lambda = 0$, this suggests trait evolution is independent of phylogenetic
229 association, which is equivalent to generalized least square (GLS) model. We also assessed the
230 evolutionary contexts of morphological traits with maximum-likelihood ancestral state
231 reconstruction using ‘fastAnc’ function in Phytools (Revell, 2012).

232 For the species that lacked molecular data, we added them as polytomous tips to the node
233 representing the latest common ancestor on the tree. We then generated 100 random trees with
234 randomly resolved polytomous tips. Each new node was added using the function ‘multi2di’
235 (package ‘ape’; Paradis et al. 2004), and was given a branch length that was randomly drawn
236 from a normal distribution of branch lengths with a mean of $0.1 \times$ mean branch lengths of the
237 original tree, and a standard deviation of $0.01 \times$ the standard deviation of branch lengths from the
238 original tree.

239 We analyzed phylogenetically-justified correlations using phylogenetic generalized least
240 square (PGLS) analyses (package ‘caper’; Orme et al., 2013). For each correlation, we ran PGLS
241 on all random trees and summarized the results (ML λ and coefficients), which were then
242 compared with those from ordinary generalized least square (GLS) tests conducted without
243 referring to the phylogeny (i.e., $\lambda = 0$). To avoid zero-inflation in correlational analyses due to
244 winglessness (i.e., Q = 0), we used two methods for correlations involving Q: (1) excluding
245 species with Q = 0; and (2) converting Q to a pseudo-continuous ordinal variable as: 1 (Q = 0), 2
246 ($0 < Q < 0.3$), 3 ($0.3 < Q < 0.6$), or 4 ($Q > 0.6$; see Symonds and Blomberg, 2014). Also, we
247 adopted a similar protocol for all correlations involving ΔQ , whereby ΔQ was converted to: 1
248 ($\Delta Q < 0$), 2 ($\Delta Q = 0$), 3 ($0 < \Delta Q < 0.3$), 4 ($0.3 < \Delta Q < 0.6$), or 5 ($\Delta Q > 0.6$). In addition, to
249 accommodate the bimodal distribution of Q (see Results), we categorized short-wing and a long-
250 wing insect groups as ‘0’ and ‘1’ and applied logistic regression models separately. We defined
251 short vs. long winged based on the distribution of Q values across all species (see the dotted line
252 in Fig. 3b).

253

254

255 **3. Results**

256

257 **Sex-specific variation in flight-related morphology**

258 Among all sampled insects, ~44% of females and ~51% of males were winged. Relative wing
259 size (Q) varied continuously from complete winglessness ($Q = 0$) to fully-sized wings (i.e., $Q \approx$
260 0.85; **Fig. 3a,b**). For both sexes, the relative frequency of Q was bimodally distributed with a
261 valley near $Q = 0.3$, and two peaks near $Q = 0.1$ and $Q = 0.7$, respectively. Variation in the
262 bimodal distribution was sex-specific, whereby the majority of males exhibited medium- to
263 fully-sized wings (i.e., $Q > 0.4$) whereas most females exhibited either medium- to fully-sized
264 wings or miniaturized wings ($Q < 0.3$). The frequency distribution of body length (L) was bell-
265 shaped, with females exhibiting a wider range and greater mean length compared to males (male
266 range: 17 mm – 190 mm, female range: 12.6 mm – 285 mm; male mean: 69.2 mm, female mean:
267 87.1 mm; see **Fig. 3c**). In both sexes, the median body length of wingless group was greater than
268 that of the winged group. The GLS regression model suggested significant inverse correlation
269 between Q and L in long-wing males but not in other groups (**Fig. 3d,e**).
270

271 At the species level, extent of SWD varied with wing size. Of 183 winged species with data
272 from both sexes, ~57% (88 species) showed various levels of male-biased SWD ($\Delta Q > 0$; **Fig.**
273 **3f**). Female-biased SWD, however, tended to be found in species for which both sexes possessed
274 long wings. Of the other 42% of species with female-biased SWD ($\Delta Q < 0$), most exhibited long
275 wings ($Q > 0.6$ in both sexes). In general, phasmids showed different combinations of a
276 continuously varying SWD and female-biased SSD (**Fig. 3g**). For *A. tanarata* group, the
277 reduction in coefficients of wing and body size toward higher altitudes was sex-specific (**Fig.**
278 **3d,e**). Males showed a relatively higher extent of wing reduction, leading to a reversal of SWD
279 from male- to female-biased (**Fig. 3g**).
280

281 **Sex-specific flight reduction**

282 Scaling of wing area with wing length was nearly isometric, with an exponent (b) of
283 approximately 1.84 in both sexes (**Fig. 4a**). The allometric scaling of insect mass with respect to
284 body length was, however, sex-dependent, with females exhibiting a higher slope coefficient and
285 scaling exponent relative to males (**Fig. 4b**). Larger female phasmids thus have
286 disproportionately greater mass. Consequentially, the allometric coefficient for wing loading in
287 females was ~2.9 greater than that of males (**Eqn. 4**; **Fig. 4c,d**); females generally have much
288 greater wing loading and potentially greater loss of aerodynamic capability when compared to
289 males of the same relative wing size. Notably, the male of *Heteropteryx dilatata*, a
290 morphological outlier with full-sized forewings, showed higher wing loading than other males
291 due to disproportionately greater body mass. If selection favors lower wing loading and better
292 flight in both sexes, it is then possible to assess consequences of the evolution of female-biased
293 SWD. Based on the regression models of **Eqn. 7**, the ratio of female wing size (Q_F) to that of
294 male's (Q_M) can be expressed as:

$$295 r_Q = \frac{Q_F}{Q_M} = \exp(b^{-1} \ln(r_C)) \quad (9)$$

296 where $r_C = C_F/C_M$ is the ratio of the slope coefficient between two sexes. Given that $r_C = 2.89$
297 and $b = 1.84$ (**Table 1**), then r_Q equals 1.78, suggesting that Q_F should be 78% greater than

299 Q_M to attain the same wing loading (**Fig. 4e**). This outcome may partially underlie the high
300 frequency of female-biased SWD found in long-winged taxa (see Discussion).

301
302 Variation in wing loading can also be presented as a three-dimensional landscape relative
303 to wing and body size. The allometric effect is stronger in females, whereas males exhibit a
304 smaller lower boundary for wing loading (**Fig. 5a,b**). Projecting the species richness distribution
305 onto these landscapes demonstrates clustering of taxa on the wing loading functional landscape
306 (**Fig. 5c,d**). Both sexes showed two major clusters associated with low and high wing loadings,
307 corresponding to long-winged and miniaturized-wing morphologies, respectively. The majority
308 of long-winged females were allometrically constrained to values of wing loading between $10^{-0.5} \text{ Nm}^{-2} < p_w < 1 \text{ Nm}^{-2}$, whereas long-winged males clustered near a value of 10^{-1} Nm^{-2} , with a
309 number of taxa characterized by even lower values. The miniaturized-wing taxa in both sexes
310 tended to concentrate within the high wing loading regime (i.e., $p_w > 10 \text{ Nm}^{-2}$). Despite sexual
311 differences in the topology of wing loading landscape, a threshold wing loading between $1 \text{ Nm}^{-2} < p_w < 10 \text{ Nm}^{-2}$ was associated with the largely unoccupied region of phenotypic space ($Q = 0.3$;
312 **Fig. 3b**).
313
314

315 316 **Wing size-dependent evolutionary correlations**

317 Our tree topology and estimates of diversification times were largely concordant with those
318 of published phasmid phylogenies (see Whiting et al. 2003; Bradler et al. 2015; Robertson et al.
319 2018; **Fig. 6**; **Supplementary Fig. S2**). Within *A. tanarata* group, the divergence time between
320 the lowland subspecies (*A. tanarata singapura*) and two highland subspecies was ~3 Myr ago,
321 while the divergence time between two highland subspecies was ~1 Myr ago. Significant
322 phylogenetic signal was present in all morphological traits (**Table 2**). Our conservative ancestral
323 state reconstruction showed high evolutionary lability of wing and body size, and suggested an
324 intermediate wing size ($Q < 0.4$) preceded various levels of gains and losses in both sexes
325 (**Supplementary Fig. S4**).
326
327

328 Based on PGLS results, there was a significant inverse correlation between Q and L in
329 long-wing insects ($Q > 0.33$) of both sexes (**Fig. 7a,b; Table 3**), which supported our initial
330 hypothesis on evolutionary coupling between wing and body size. In addition, sex-averaged
331 body size was coupled with the extent of both SWD and SSD in long-wing species ($Q > 0.33$ in
332 both sexes), suggesting opposite trends of variation in SWD and SSD along the gradient of sex-
333 averaged body size (**Fig. 7c**). An exemplar of this correlation is demonstrated in **Fig. 7d** and e,
334 whereby increases in SSD and SWD both lead to greater sexual differences in wing loading.
335 Short-wing insects generally lacked significant correlation between wing and body size (**Fig.**
336 **7a,c**). Across all winged species, variation in female traits contributed more substantially to
337 intersexual differences, as shown by the predominant roles of female Q and L values in
338 determining variation in SWD and SSD, respectively (**Supplementary Fig. S6, Table S2**).
339
340

341 **4. Discussion**

342
343 Most winged phasmid species possess either small or large wings (**Fig. 3b**). Few species have
344 intermediate-sized wings, suggesting the presence of a fitness valley defined by two ‘adaptive
345 peaks’ (see Stroud and Losos, 2016): one peak consists of wingless taxa and those with
346 miniaturized-wings (i.e., $Q < \sim 0.3$), and another represents volant taxa (i.e., $Q > \sim 0.6$). Insects
347 with wing size near $Q = \sim 0.3$ are likely caught in transition between these two forms, with
348 greater probability of either gaining or losing wing size, depending on the interplay between
349 various selective forces (see below). The predominance of wingless species in phasmids may in
350 part derive from reduced dispersal capacity leading to population isolation and ultimately genetic
351 divergence. Given the possibility that repeated gain and losses of flight are associated with
352 species diversification (Goldberg and Igić, 2008), the linkage of evolutionary transitions between
353 winged and wingless forms with diversification rates and overall macroevolutionary patterns
354 should be addressed in future comparative studies of the group. The significant wing size
355 reduction over relatively short divergence time, as in *A. tanarata* group, further demonstrates that
356 the evolution of flightlessness is recurrent and occurs within nominal species. Similar wing size
357 reduction scenario has been reported in alpine stoneflies (McCulloch et al., 2016). The evolution
358 of flight-related morphology in phasmids can, in part, be viewed as displacement on the wing
359 loading landscape (**Fig. 8a**), reflecting effects of dual variation in wing and body size. This
360 multidimensional view provides a more complete perspective than consideration of wing size
361 alone (as otherwise indicated by the inset arrows of **Fig. 8a**).
362

363 Flight in general enhances resource acquisition, dispersal, and escape from predators
364 (Dudley, 2000), but wings can readily be lost in evolutionary time, or co-opted for non-
365 aerodynamic purposes. Wing reduction in insects often derives from trade-offs with fecundity in
366 particular contexts (e.g., habitat persistence, colonization of high-altitude environments;
367 see Roff, 1994), whereas miniaturized and aerodynamically irrelevant wings often associate with
368 derived defensive functions (e.g., startle displays and stridulation; Robinson, 1968; **Fig. 8b**;
369 **Supplementary Table S3**). Altitudinal changes in life history strategies likely contribute to both
370 body size miniaturization and wing reduction, as in the *A. tanarata* clade (**Fig. 2b**). For high-
371 altitude species more generally, lower plant canopies at high elevations may reduce the
372 functional significance of flight. By contrast, phasmid species with high dietary specificity might
373 experience stronger selection for flight performance (e.g., Blüthgen et al., 2006). No data are
374 presently available on flight abilities and associated aerodynamics among phasmid species.
375

376 For long-wing stick insects, aerial mobility may be an important component in sexual
377 selection for enhanced male locomotor performance. Female phasmids tend to be less mobile and
378 inconspicuous, whereas greater mobility in males may allow for greater success in dispersal and
379 mating. The inverse correlation between wing and body size in male stick insects (**Fig. 7a,b**)
380 suggests that selection for flight has limited the evolution of larger body size. Similar selection
381 on male mobility and an enhanced locomotor apparatus has been documented in other male
382 insects (Kelly et al., 2008). In wingless and short-wing species, larger body size might make a
383 species more competitive in male-male competition (see Sivinski, 1978). A developmental
384 tradeoff may limit the evolution of wing size, as shown by the inverse correlation between
385 mating success and flight capability (e.g., in Orthopteran and Hemipteran insects; Fujisaki, 1992;
386 Crnokrak and Roff, 1995; Fairbairn and Preziosi, 1996). Future studies may compare the

387 variation of male body size between winged and wingless clades to test whether the evolution of
388 male body size is constrained by selection for flight.
389

390 Sexual differences in mass allometry and body size are key factors influencing the
391 evolution of phasmid wing dimorphism. Selection for increased fecundity will favor wing
392 reduction in females, which can then lead to male-biased SWD as well as the evolution of
393 defensive mechanisms that do not rely on flight; strong selection for flight capability may lead to
394 female-biased SWD. Large female wings may be specifically favored in winged species with
395 aerial copulation (e.g., *Trachythorax* spp.). Female-biased SSD is likely a canalized feature in
396 orthopteroid insects, more generally (see Bidau et. al., 2016). In winged stick insects, the degree
397 of SSD is clearly influenced by fecundity selection in females and flight selection in males. The
398 allometric variation in SSD (i.e., the inverse correlation between ΔL and sex-averaged L ; see
399 **Fig. 7c,d**) is consistent with Rensch's Rule (i.e., females are disproportionately larger in large
400 species; Abouheif and Fairbairn, 1997; Fairbairn, 1997; Teder and Tammaru, 2005), instead of
401 the converse outcome (i.e., isometric scaling in both sexes). This result may, however, be biased
402 by allometric changes in body shape. For example, many phasmid species exhibit
403 disproportionately slender bodies that may mimic plant stems, whereas other species have
404 evolved thickened bodies for defense (e.g., the 'tree lobster' ecomorph; Buckley et al., 2008). In
405 scaling of wing loading (**Fig. 4d**), the contrast between *H. dilatata* male (family
406 Heteropterygidae) and other insects (mostly in the subfamily Necrosciinae) suggested clade-
407 specific allometry scaling. Future comparative assessment of body segment shapes and masses,
408 in addition to body length, would enhance our understanding of allometric variation in SSD
409 among phasmid taxa.
410

411 In winged phasmids, SSD and SWD are significantly correlated but not within either short-
412 or long-wing species (**Fig. 7c**; **Supplementary Fig. S3**), reflecting the interaction between
413 multiple selective forces within sex-specific ecological contexts (**Fig. 8a**). The evolutionary
414 intercorrelation between SSD and SWD is generally underexplored for most other insects.
415 Pterygote insects in general exhibit various types of SWD (e.g., male-biased and female-biased
416 SWD have been reported in at least 11 and 5 orders, respectively; see Thayer, 1992), which can
417 be correlated with sex-specific flight ecology (e.g., flight height and behavior; see DeVries et al.,
418 2010) and sexual selection for flight capability (e.g., copulation flight in caddisfly; Gullefors and
419 Petersson, 1993). Future studies may address clade-specific SWD by correlating aforementioned
420 factors within phylogenetic contexts.
421

422 These results for stick insects may provide more general insight into evolutionary
423 transitions between wingless and fully winged insects. Given the widespread secondary loss of
424 flight in pterygotes, sex-specific morphological scaling along the wing loading landscape can
425 indicate the possible utility of partially reduced wings. Aerodynamic use of reduced wings
426 during descent may be expected in arboreal pterygotes undergoing wing reduction, whereas non-
427 aerodynamic functions would be predicted to be more likely in non-arboreal taxa (e.g.,
428 stridulatory wings in ground-dwelling insects). The eventual loss of aerodynamic utility may be
429 characterized by a threshold wing loading (i.e., between $1 \text{ Nm}^{-2} < p_w < 10 \text{ Nm}^{-2}$ as in stick
430 insects), beyond which point selection for aerodynamic utility become insignificant. Similarly,
431 morphological evolution associated with the origin of wings and of insect flight may have been
432 sexually dimorphic, particularly if the earliest winglets served a non-aerodynamic function such

433 as visual display (Alexander and Brown, 1963), with subsequently increases in size and mobility
434 for aerial behaviors (see Dudley, 2000; Dudley and Yanoviak, 2011). Reductions in body size
435 (with concomitantly lower wing loadings) may also favor the evolution of flight, as characterized
436 the lineage leading to birds (Lee et al., 2014; Xu et al., 2014). Allometric variation in body
437 structures can occur on both developmental and macroevolutionary timescales, and likely
438 interacts with selection on aerodynamic performance. For example, if ancestral pterygotes
439 retained winglets across nymphal instars, then selection for lower wing loading would foster
440 allometric increases in wing size as well as a reduction in mass allometry (with less influence of
441 body size growth to wing loading; **Fig. 5**). Physical models with wings of different sizes can be
442 used to test biomechanical consequences of such differential allometries, as constrained by
443 relevant morphologies inferred from the fossil record. And for extant phasmids, assessment of
444 flight behaviors and aerial capacity across taxa is now clearly warranted.
445

446 **Author contributions:** Y.Z. devised experiments and performed the majority of data collection
447 and analyses. C.O. and S.P. participated in morphological data collection. S. S. contributed to
448 molecular data collection. X. C. contributed to phylogenetic analyses. F. H. contributed to field
449 data collection of *Asceles tanarata* group. All authors contributed to writing of the manuscript.

450 **Acknowledgments:** We thank Francis Seow-Choen for providing captive bred insects, helping
451 with field works, and commenting on stick insect natural history. We also thank Lynn Nguyen,
452 Camille Gonzales, Faye Pon, Joan Chen, Nina Gnong, Stephanie Yom, Yuexiang Chen,
453 Chulabush Khatancharoen, Biying Li, Grisanu Naing, Jizel Emralino, Xiaolin Chen, Ian
454 Abercrombie, Yamai Shi-Fu Huang, Azuan Aziz and Juhaida Harun for help with data
455 collection, and David Wake and Sven Bradler for comments on the manuscript. We further thank
456 Paul Brock, Nicholas Matzke and Emma Goldberg for comments at the early stage of the work,
457 and the Forestry Department of Pahang, Malaysia, for permission of insect collection. This
458 research was supported by National Science Foundation (DDIG 1110855), Museum of
459 Vertebrate Zoology, the Department of Integrative Biology at UC-Berkeley, the Undergraduate
460 Research Apprentice Program (URAP) of UC-Berkeley, the Society for Integrative and
461 Comparative Biology (SICB), and the Ministry of Higher Education Malaysia
462 (FRGS/1/2012/SG03/UKM/03/1(STWN)).

- 463 **References**
- 464
- 465 **Abouheif, E. and Fairbairn, D. J.** (1997). A comparative analysis of allometry for sexual size
466 dimorphism: assessing Rensch's rule. *Am. Nat.* **149**, 540-562.
- 467 **Alexander, R. D. and Brown Jr, W. L.** (1963). Mating behavior and the origin of insect wings.
468 *Occas. Papers Mus. Zool. Univ. Mich.* **628**, 1-19.
- 469 **Aljanabi, S. M. and Martinez, I.** (1997). Universal and rapid salt-extraction of high quality
470 genomic DNA for PCR-based techniques. *Nucleic Acids Res.* **25**, 4692-4693.
- 471 **Bidau, C. J., Taffarel, A. and Castillo, E. R.** (2016). Breaking the rule: multiple patterns of
472 scaling of sexual size dimorphism with body size in orthopteroid insects. *Rev. Soc.*
473 *Entomol. Arg.* **75**.
- 474 **Blanckenhorn, W. U.** (2000). The evolution of body size: what keeps organisms small? *Q. Rev.*
475 *Biol.* **75**, 385-407.
- 476 **Blüthgen, N., Metzner, A. and Ruf, D.** (2006). Food plant selection by stick insects (Phasmida)
477 in a Bornean rain forest. *J. Trop. Ecol.* **22**, 35-40.
- 478 **Bradler, S.** (2009). Phylogeny of the stick and leaf insects (Insecta: Phasmatodea). *Spec. Phyl.*
479 *Evol.* **2**, 3-139.
- 480 **Bradler, S., Cliquennois, N. and Buckley, T. R.** (2015). Single origin of the Mascarene stick
481 insects: ancient radiation on sunken islands? *BMC Evol. Biol.* **15**, 196.
- 482 **Brock, P.D.** (1999). *Stick and leaf insects of Peninsular Malaysia and Singapore*, Malaysian
483 Nature Society.
- 484 **Brock, P.D., Büscher, T. & Baker, E.** (2019). *Phasmida Species File Online Version 5.0*.
485 <http://phasmida.speciesfile.org>
- 486 **Buckley, T. R., Attanayake, D. and Bradler, S.** (2008). Extreme convergence in stick insect
487 evolution: phylogenetic placement of the Lord Howe Island tree lobster. *Proc. Royal Soc.*
488 *B* **276**, 1055-1062.
- 489 **Chown, S. L. and Gaston, K. J.** (2010). Body size variation in insects: a macroecological
490 perspective. *Biol. Rev.* **85**, 139-169.
- 491 **Crnokrak, P. and Roff, D. A.** (1995). Fitness differences associated with calling behaviour in
492 the two wing morphs of male sand crickets, *Gryllus firmus*. *Anim. Behav.* **50**, 1475-1481.
- 493 **DeVries, P. J., Penz, C. M. and Hill, R. I.** (2010). Vertical distribution, flight behaviour and
494 evolution of wing morphology in *Morpho* butterflies. *J. Anim. Ecol.* **79**, 1077-1085.
- 495 **Drummond, A. J., Suchard, M. A., Xie, D. and Rambaut, A.** (2012). Bayesian phylogenetics
496 with BEAUTi and the BEAST 1.7. *Mol. Biol. Evol.* **29**, 1969-1973.
- 497 **Dudley, R.** (2000). *The biomechanics of insect flight: form, function, evolution*, Princeton Univ
498 Pr.
- 499 **Dudley, R. and Yanoviak, S. P.** (2011). Animal aloft: the origins of aerial behavior and flight.
500 *Integr. Comp. Biol.* **51**, 926-936.
- 501 **Edgar, R. C.** (2004). MUSCLE: multiple sequence alignment with high accuracy and high
502 throughput. *Nucleic Acids Res.* **32**, 1792-1797.
- 503 **Fairbairn, D. J.** (1997). Allometry for sexual size dimorphism: pattern and process in the
504 coevolution of body size in males and females. *Annu. Rev. Ecol. Evol. Syst.* **28**, 659-687.
- 505 **Fairbairn, D. J. and Preziosi, R. F.** (1996). Sexual selection and the evolution of sexual size
506 dimorphism in the water strider, *Aquarius remigis*. *Evolution* **50**, 1549-1559.
- 507 **Freckleton, R. P., Harvey, P. H. and Pagel, M.** (2002). Phylogenetic analysis and comparative
508 data: a test and review of evidence. *Am. Nat.* **160**, 712-726.

- 509 **Fujisaki, K.** (1992). A male fitness advantage to wing reduction in the oriental chinch bug,
510 *Cavelerius saccharivorus* Okajima (Heteroptera: Lygaeidae). *Popul Ecol* **34**, 173-183.
- 511 **Goldberg, E. E. and Igić, B.** (2008). On phylogenetic tests of irreversible evolution. *Evolution*
512 **62**, 2727-2741.
- 513 **Grimaldi, D. and Engel, M.** (2005). *Evolution of the Insects*, Cambridge University Press.
- 514 **Gullefors, B. and Petersson, E.** (1993). Sexual dimorphism in relation to swarming and pair
515 formation patterns in *Leptocerid* caddisflies (Trichoptera: Leptoceridae). *J Insect Behav* **6**,
516 563-577.
- 517 **Hedrick, A. V. and Temeles, E. J.** (1989). The evolution of sexual dimorphism in animals:
518 hypotheses and tests. *Trends Ecol. Evo.* **4**, 136-138.
- 519 **Kelly, C. D., Bussiere, L. F. and Gwynne, D. T.** (2008). Sexual selection for male mobility in a
520 giant insect with female-biased size dimorphism. *Am. Nat.* **172**, 417-423.
- 521 **Lee, M. S., Cau, A., Naish, D. and Dyke, G. J.** (2014). Dinosaur evolution. Sustained
522 miniaturization and anatomical innovation in the dinosaurian ancestors of birds. *Science*
523 **345**, 562-566.
- 524 **McCulloch, G. A., Wallis, G. P. and Waters, J. M.** (2016). A time-calibrated phylogeny of
525 southern hemisphere stoneflies: Testing for Gondwanan origins. *Mol Phylogenet Evol* **96**,
526 150-160.
- 527 **Nel, A. and Delfosse, E.** (2011). A new Chinese Mesozoic stick insect. *Acta Palaeontol. Pol.* **56**,
528 429-433.
- 529 **Orme, D., Freckleton, R., Thomas, G. and Petzoldt, T.** (2013). The caper package:
530 comparative analysis of phylogenetics and evolution in R. *R package version 5*, 1-36.
- 531 **Pagel, M.** (1997). Inferring evolutionary processes from phylogenies. *Zool. Scr.* **26**, 331-348.
- 532 **Pagel, M.** (1999). Inferring the historical patterns of biological evolution. *Nature* **401**, 877-884.
- 533 **Paradis, E., Claude, J. and Strimmer, K.** (2004). APE: analyses of phylogenetics and
534 evolution in R language. *Bioinformatics* **20**, 289-290.
- 535 **Posada, D.** (2008). jModelTest: phylogenetic model averaging. *Mol. Biol. Evol.* **25**, 1253-1256.
- 536 **Rambaut, A., Drummond, A. J., Xie, D., Baele, G. and Suchard, M. A.** (2018). Posterior
537 summarization in Bayesian phylogenetics using Tracer 1.7. *Syst. Biol.* **67**, 901-904.
- 538 **Rasnitsyn, A. P. and Ross, A. J.** (2000). A preliminary list of arthropod families present in the
539 Burmese amber collection at The Natural History Museum, London. *Bull. Mus. Nat.
540 Hist. Geol.* **56**, 21-24.
- 541 **Revell, L. J.** (2012). phytools: an R package for phylogenetic comparative biology (and other
542 things). *Methods Ecol. Evol.* **3**, 217-223.
- 543 **Robertson, J. A., Bradler, S. and Whiting, M. F.** (2018). Evolution of oviposition techniques
544 in stick and leaf insects (Phasmatodea). *Front. Ecol. Evo.* **6**, 216.
- 545 **Robinson, M. H.** (1968). The defensive behavior of *Pterinoxylus spinulosus* Redtenbacher, a
546 winged stick insect from Panama (Phasmatodea). *Psyche (Camb. Mass.)* **75**, 195-207.
- 547 **Roff, D. A.** (1986). The evolution of wing dimorphism in insects. *Evol.* 1009-1020.
- 548 **Roff, D. A.** (1990). The evolution of flightlessness in insects. *Ecol. Monogr.* 389-421.
- 549 **Roff, D. A.** (1994). The evolution of flightlessness: is history important? *Evol. Ecol.* **8**, 639-657.
- 550 **Schneider, C. A., Rasband, W. S. and Eliceiri, K. W.** (2012). NIH Image to ImageJ: 25 years
551 of image analysis. *Nat. Methods* **9**, 671.
- 552 **Sellick, J. T. C.** (1994). Phasmida (stick insect) eggs from the Eocene of Oregon. *Palaeontol.*
553 **37**, 913-922.

- 554 **Seow-Choen, F. and Brock, P.** (1999). *Stick and Leaf Insects of Peninsular Malaysia and*
555 *Singapore*, Malaysian Nature Society.
- 556 **Shang, L., Béthoux, O. and Ren, D.** (2011). New stem-Phasmatodea from the middle Jurassic
557 of China. *Eur. J. Entomol.* **108**, 677.
- 558 **Shine, R.** (1989). Ecological causes for the evolution of sexual dimorphism: a review of the
559 evidence. *Q. Rev. Biol.* **64**, 419-461.
- 560 **Sivinski, J.** (1978). Intrasexual aggression in the stick insects *Diapheromera veliei* and *D.*
561 *covilleae* and sexual dimorphism in the Phasmatodea. *Psyche (Camb. Mass.)* **85**, 395-405.
- 562 **Stone, G. and French, V.** (2003). Evolution: Have Wings Come, Gone and Come Again?
563 *Current Biology* **13**, 436-438.
- 564 **Stroud, J. T. and Losos, J. B.** (2016). Ecological opportunity and adaptive radiation. *A Annu.*
565 *Rev. Ecol. Evol. Syst.* **47**, 507-532.
- 566 **Symonds, M. R. and Blomberg, S. P.** (2014). A primer on phylogenetic generalised least
567 squares. In *Modern phylogenetic comparative methods and their application in*
568 *evolutionary biology*, pp. 105-130. Springer.
- 569 **Teder, T. and Tammaru, T.** (2005). Sexual size dimorphism within species increases with body
570 size in insects. *Oikos* **108**, 321-334.
- 571 **Thayer, M. K.** (1992). Discovery of sexual wing dimorphism in Staphylinidae (Coleoptera): "Omalium" flavidum, and a discussion of wing dimorphism in insects. *Journal of the New York Entomological Society* , 540-573.
- 572 **Trueman, J. W. H., Pfeil, B. E., Kelchner, S. A. and Yeates, D. K.** (2004). Did stick insects
573 really regain their wings? *Syst. Entomol.* **29**, 138-139.
- 574 **Wang, M., Béthoux, O., Bradler, S., Jacques, F. M., Cui, Y. and Ren, D.** (2014). Under cover
575 at pre-angiosperm times: a cloaked phasmatodean insect from the Early Cretaceous Jehol
576 biota. *PLoS One* **9**, e91290.
- 577 **Wedmann, S., Bradler, S. and Rust, J.** (2007). The first fossil leaf insect: 47 million years of
578 specialized cryptic morphology and behavior. *Proc. Natl. Acad. Sci. U.S.A* **104**, 565-569.
- 579 **Whiting, M. F., Bradler, S. and Maxwell, T.** (2003). Loss and recovery of wings in stick
580 insects. *Nature* **421**, 264-267.
- 581 **Whiting, M. F. and Whiting, A. S.** (2004). Is Wing Recurrence really impossible?: a reply to
582 Trueman et al. *Syst. Entomol.* **29**, 140-141.
- 583 **Xu, X., Zhou, Z., Dudley, R., Mackem, S., Chuong, C. M., Erickson, G. M. and Varricchio,**
584 **D. J.** (2014). An integrative approach to understanding bird origins. *Science* **346**,
585 1253293.
- 586
- 587
- 588
- 589
- 590
- 591

592 **Figure captions**

593

594 **Figure 1. Diversity of flight morphology in stick insects as shown by variation in wing and**
595 **body size.** (a) Examples of insects with different sized wings; white line segments indicate
596 hindwing length. (b) Spectrum of interspecific variation in body and wing size for representative
597 species. (Photo of *Planispectrum hainanensis* courtesy of Chao Wu.)

598

599 **Figure 2. Sexual wing dimorphism (SWD) in stick insects.** (a) Representative combinations of
600 variable wing size and SWD: (1) low SWD with long wings in both sexes, (2) extreme SWD
601 with long wings in males only, and (3) low SWD with short wings in both sexes. (b) Variation in
602 wing and body sizes for the *Asceles tanarata* species group, for which SWD transitions from
603 male- to female-biased with increasing altitude. (c) Schematic demonstration of variations in
604 SWD with respect to body size and male wing size; numbers denoting taxa depicted in (a) and
605 (b). The gray arrow indicates elevational changes with increasing altitude in the *A. tanarata*
606 group.

607

608 **Figure 3. Variations in wing and body size among stick insect species.** (a) Number of winged
609 and wingless species, as grouped by the two sexes. (b) Relative frequency distribution and
610 density (of relative wing size (Q) for winged insects. The vertical dashed lines indicate a region
611 of phenotypic space that few species occupy. (c) Relative frequency distribution of body size (L).
612 Black dashed lines denote median values. (d) – (e) Scatter plots of Q versus L for winged stick
613 insects, indicating bimodal distributions. The color of overlaid hexagons represents the number
614 of species, as scaled by the heat map inset. Insets show results of generalized least squares (GLS)
615 regression models (trend line with 95% C.I.) for short- and long-wing insects, as divided by the
616 cutoff Q defined in (a). An inverse correlation between Q and L is found in long-wing males. (f)
617 Scatter plot of female wing size versus male wing size ($N = 183$ species). The color of overlaid
618 hexagons represents the number of species for each parameter combination. The majority (80%)
619 of female-biased SWD (i.e., the area above the dashed line) is associated with medium-length to
620 long wings ($Q_F > 0.5$), as indicated by the increasing density of female-biased SWD in long wing
621 females ($Q > 0.4$) (inset). (g) Scatter plot of SWD index versus SSD index, showing the
622 predominance of female-biased SSD and continuous variation in SWD (57% male-biased and
623 43% female-biased). For (d), (e), and (g), the three dark dots represent subspecies of the *A.*
624 *tanarata* group, showing sex-specific trends of wing and body size reduction with increasing
625 altitude (as indicated by arrows).

626

627 **Figure 4. Scaling of flight-related morphology.** (a) Near-isometric scaling of wing area with
628 wing size. Trend lines are based on linear regression models with slopes equal to 1.84 ± 0.05 and
629 1.84 ± 0.07 (mean \pm s.e.m.) for males and females, respectively; $R^2 = 0.98$ and $P < 0.0001$ for both
630 sex groups). (b) Allometric scaling of insect body mass with body length. Trend lines are based
631 on linear regression models; Males: slope = 1.84 ± 0.16 , $R^2 = 0.86$, $P < 0.0001$, females: slope =

632 2.39 ± 0.21 , $R^2 = 0.86$, $P < 0.0001$. (c) – (d) Allometric scaling of wing loading (p_w) in females
633 and males, respectively. Colored dots represent insects for which body mass and wing area were
634 directly measured. Gray dots are estimates based on wing and body lengths using regression
635 models (see Methods). Trendlines are based on a logistic fit. The regression model for males
636 omitted *Heteropteryx dilatata* (dark gray dot), which is a morphological outlier with well-
637 developed forewings. (e) Comparison of the scaling of p_w with respect to Q between two sexes,
638 showing that disproportionately longer wings in females are required to attain wing loading
639 equivalent to that of males.

640

641 **Figure 5. Sex-specific landscapes of wing loading relative to dimorphism and body length**
642 **among phasmid species.** Fig. 5a and Fig. 5b, wing loading relationships for females and males,
643 respectively between the two sexes; females typically have higher wing loading than males and
644 stronger allometric effects relative to body length. Fig. 5c and Fig. 5d, contours of the wing
645 loading landscape for females and males, respectively, as overlaid with hexagonal bins for
646 species counts (Fig. 3d); wing loading distribution differs substantially between the sexes.
647

648

649 **Figure 6. Phylogenetic relationships among sampled taxa, with flight-related morphology**
650 **annotated on tree tips.** Tree topology is based on concatenated COI, COII, H3 and 28S data
651 (see Methods), and branch lengths are proportional to time since divergence (in millions of
652 years). Tree is pruned to show a selection of species with data from both sexes (see
Supplementary Fig. S2 for the complete tree).

653

654 **Figure 7. Phylogenetic correlations between wing and body size among stick insect species.**
655 (a) An inverse correlation between wing and body size was found in both sexes of long-wing
656 species ($Q > 0.3$ in both sexes), indicated graphically in (b) as a coupled transition between
657 different states of wing and body size on the wing loading landscape. (c) In long-wing species,
658 sex-average L is significantly correlated with ΔL and ΔQ , demonstrated graphically in (d) as an
659 increasing sex-averaged L associated with decreasing SSD and increasing SWD. (e) Schematic
660 scenario for consequences of increased sexual dimorphism in flight-related morphology;
661 increases in female-biased SSD and male-biased SWD lead to greater difference in flight
662 performance (i.e., changes in the z-position on the wing loading landscape). Details of the PGLS
663 results are provided in Table 3.

664

665 **Figure 8. A summary of evolution of flight-related morphology in stick insects.** (a)
666 Schematic demonstration showing that the evolution of flight morphology (for any given
667 position on the wing loading landscape) is driven by the interplay between three major forces
668 and tradeoffs (inset). (b) Variation of wing utility with respect to wing size. Continuous variation
669 in aerodynamic performance is coupled with the full spectrum of wing size variation, whereas
670 derived functions such as use in startle displays or stridulation are frequently found in
671 miniaturized wings. Examples of startle display: (i), *Diesbachia hellotis* female; (ii), *Achrioptera*

672 *manga* male; (iii), *Parectatosoma* cf. *hystrix* male; (iv) *Oxyartes dorsalis* female (Photos of (i) –
673 (iii) courtesy of Bruno Kneubühler). Example of defensive stridulation: *Haaniella echinata* male.

674

676

675

677 **Tables**

678
679
680

Sex	C ₁	C ₂	a	b
Male	-2.08 (0.14)	-0.24 (0.03)	1.84 (016)	1.84 (0.06)
Female	-2.09 (0.19)	-0.16 (0.04)	2.38 (0.22)	1.84 (0.07)

681
682 **Table 1.** Comparison of coefficients for the power-law scaling of wing loading relative to wing
683 size (see Eqn. 4 and 5). Values are means with 1 s.e. in brackets. C₁ and a are slope coefficient
684 and exponent for the allometric scaling of body mass, respectively; C₂ and b are slope coefficient
685 and exponent for the scaling of wing area with wing length, respectively.
686
687
688

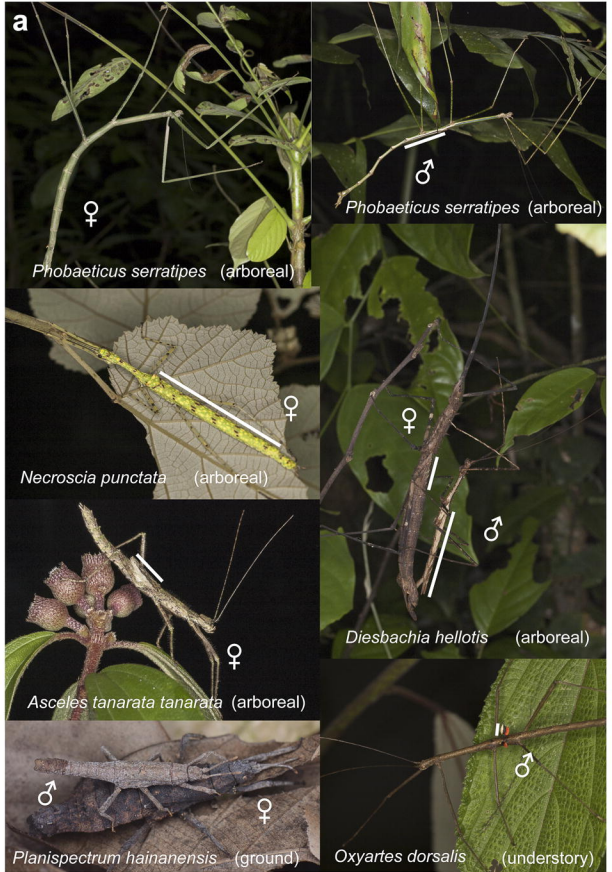
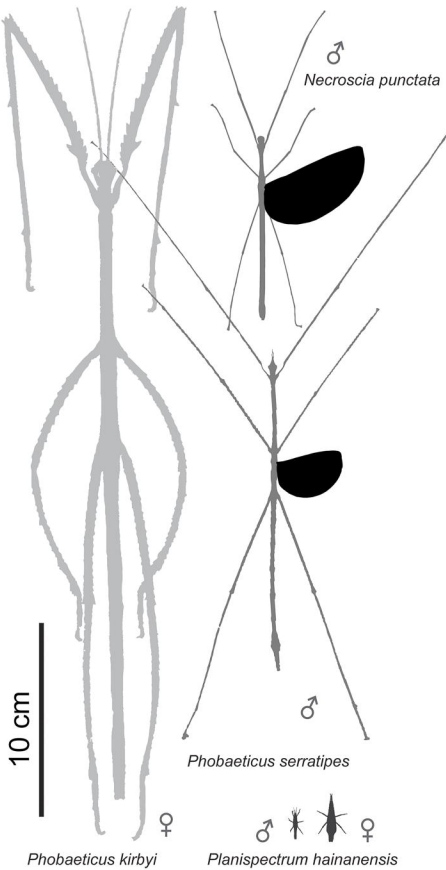
PGLS vs. GLS								
	Variable	N	ML λ	L _h (PGLS)	L _h (GLS)	L _h (PIC)	LR	P
Male	Q _M	533	1.001	293.3	-111.9	227.5	-810.3	< 0.0001
	Log ₁₀ (L _M)	533	0.922	317.9	108.9	-91.4	-418	< 0.0001
Female	Q _F	597	1.001	401.1	-100.4	292.7	-1002.9	< 0.0001
	Log ₁₀ (L _F)	597	0.916	271.8	76.1	-140.1	-391.4	< 0.0001
Species-wise comparison	Sex-average L	367	0.967	-1701.9	-1846.7	-1920.5	-289.5	< 0.0001
	ΔL	367	0.576	442.9	431.4	88.6	-23	< 0.0001
	Sex-average Q	367	0.949	114.5	-59.1	137.2	-347.2	< 0.0001
	ΔQ	367	0.926	12.6	-60.2	-3.5	-145.6	< 0.0001

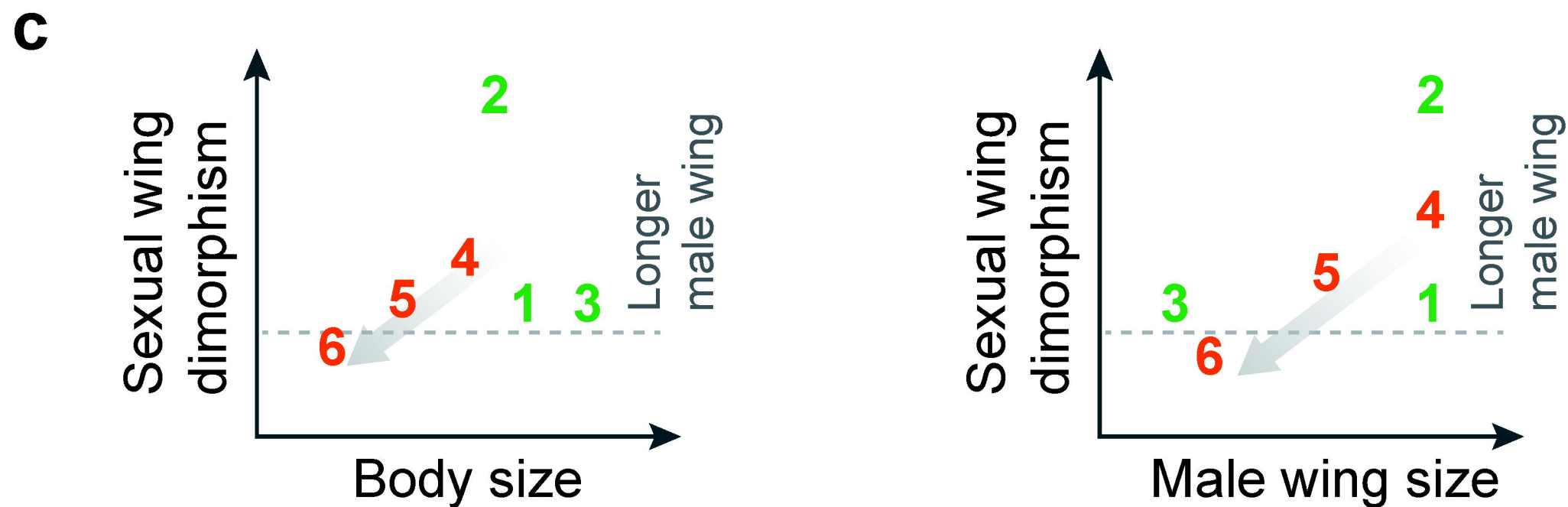
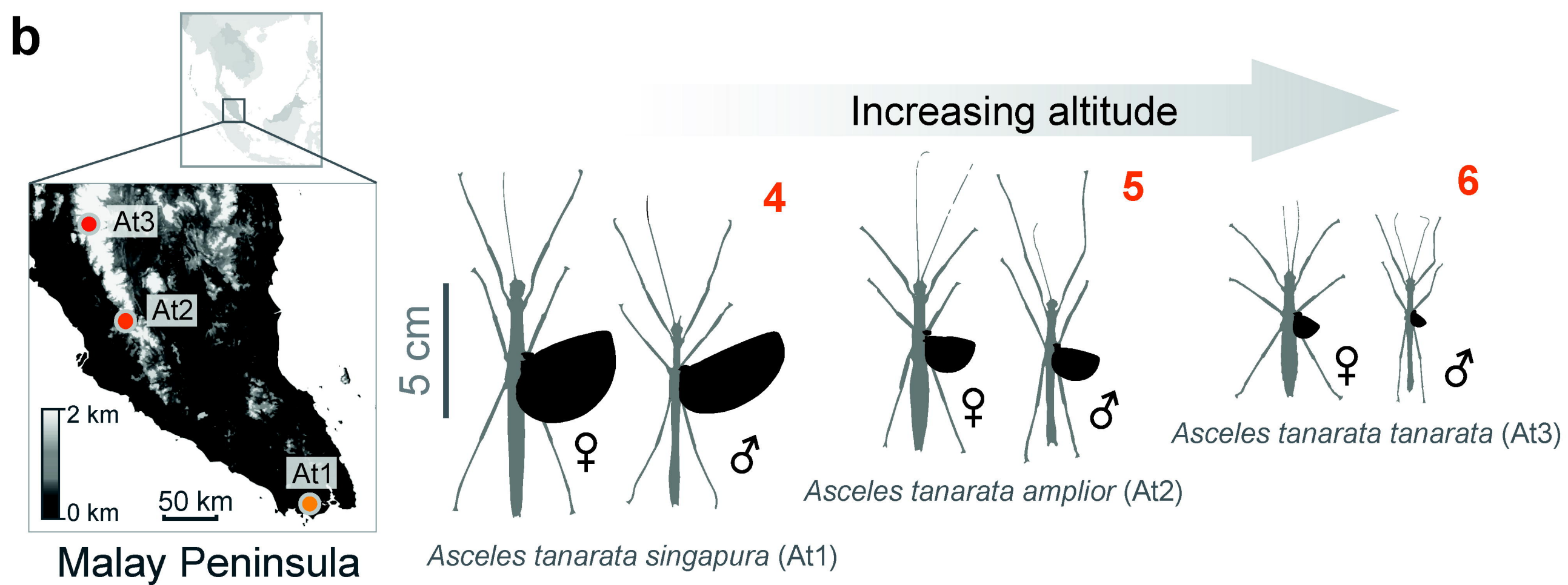
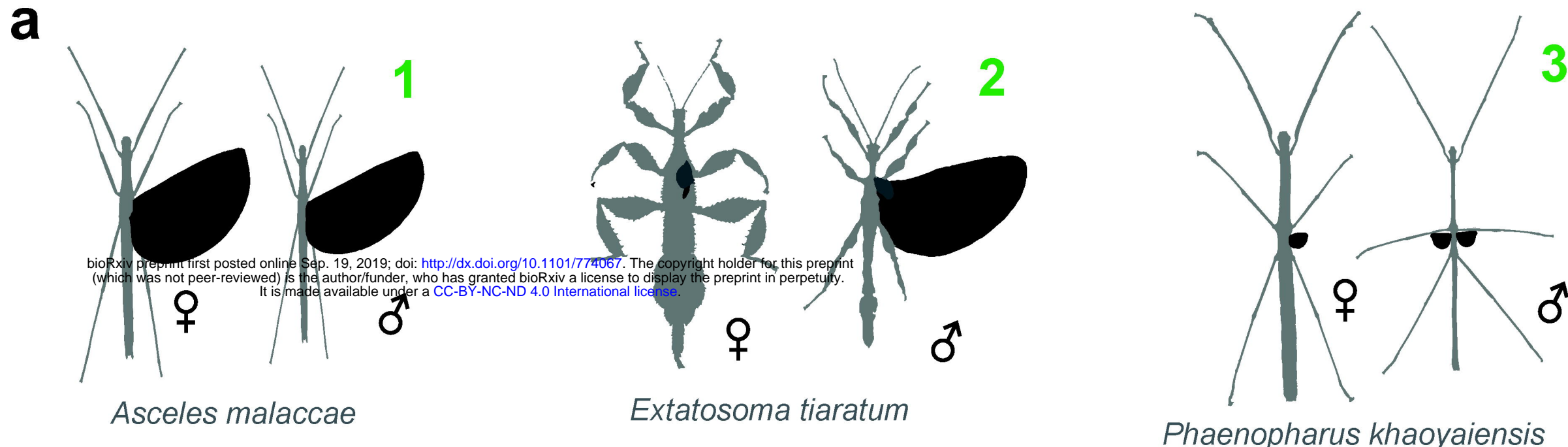
689
690
691 **Table 2.** Summary of statistical results for best model fits, comparing phylogenetic generalized
692 least squares (PGLS) models (λ estimated by maximum likelihood, ML) with generalized least
693 square (GLS) models ($\lambda = 0$) for log-transformed body length (i.e., log₁₀ L) and relative wing
694 size (Q). Species-wise traits were analyzed for all taxa using available data for both sexes.
695
696

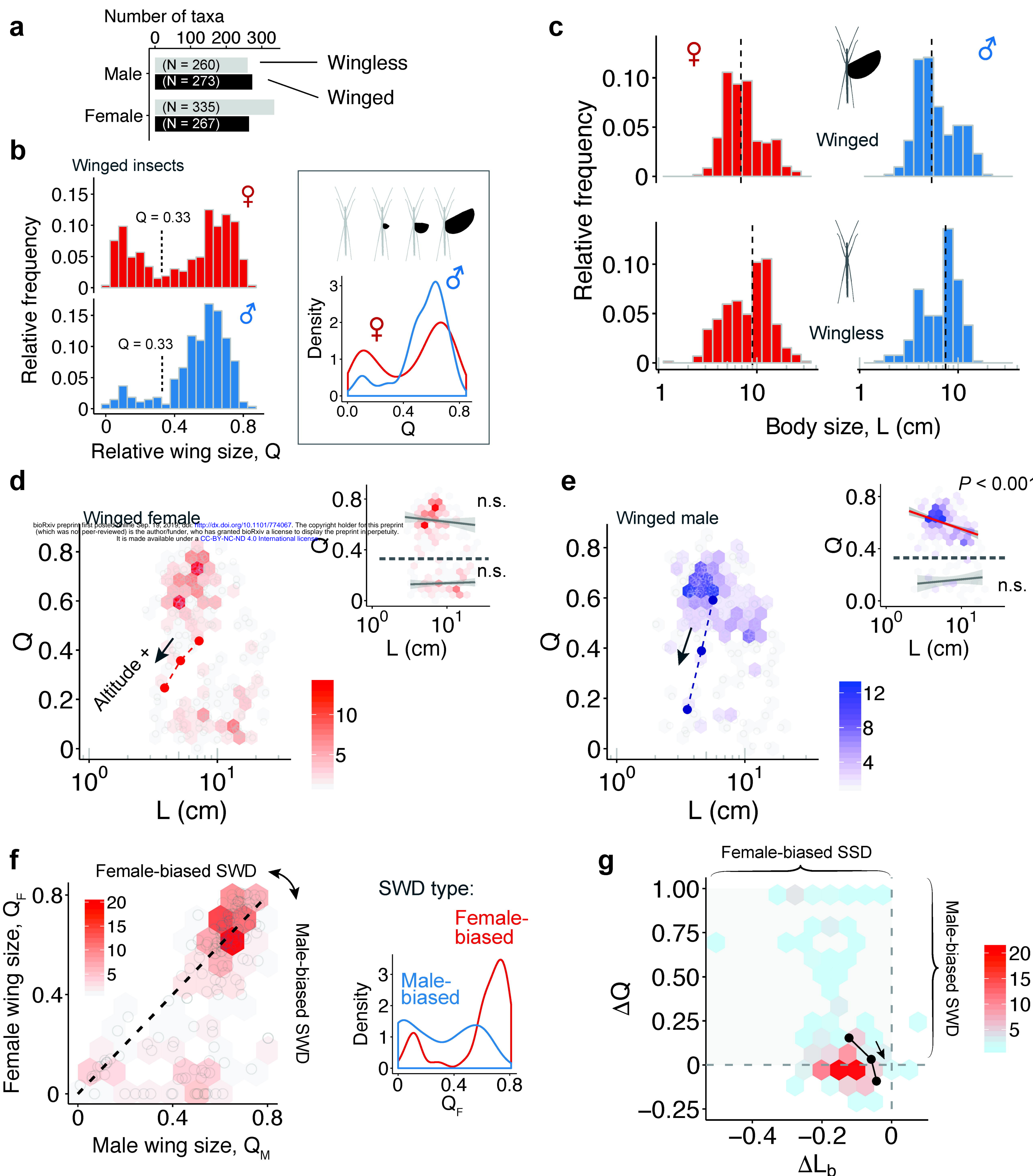
697

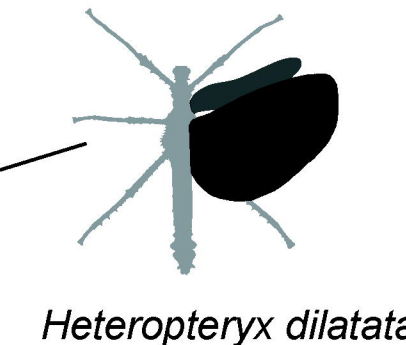
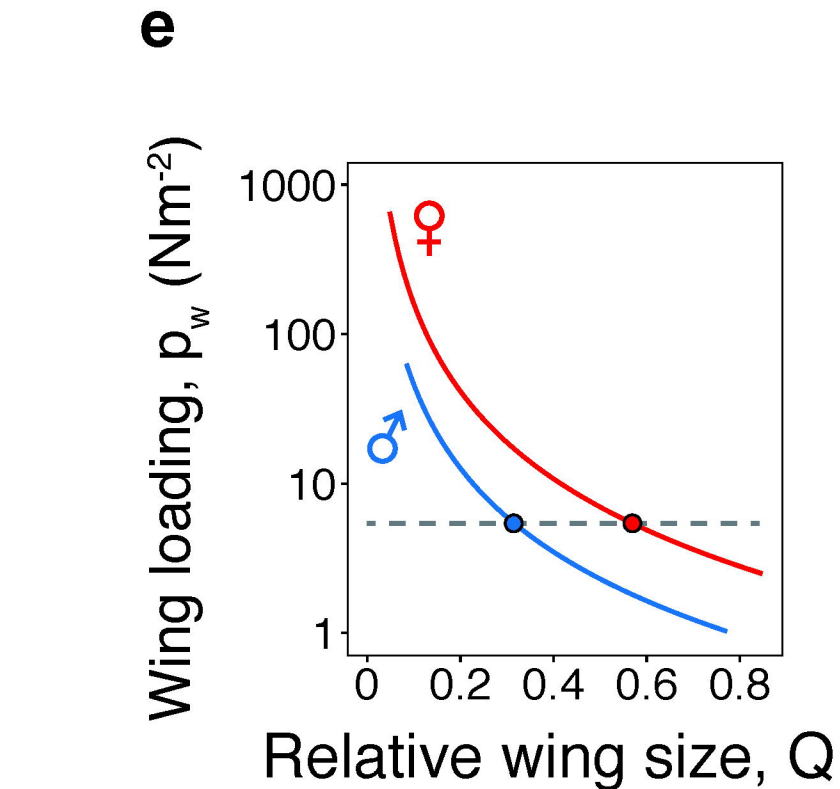
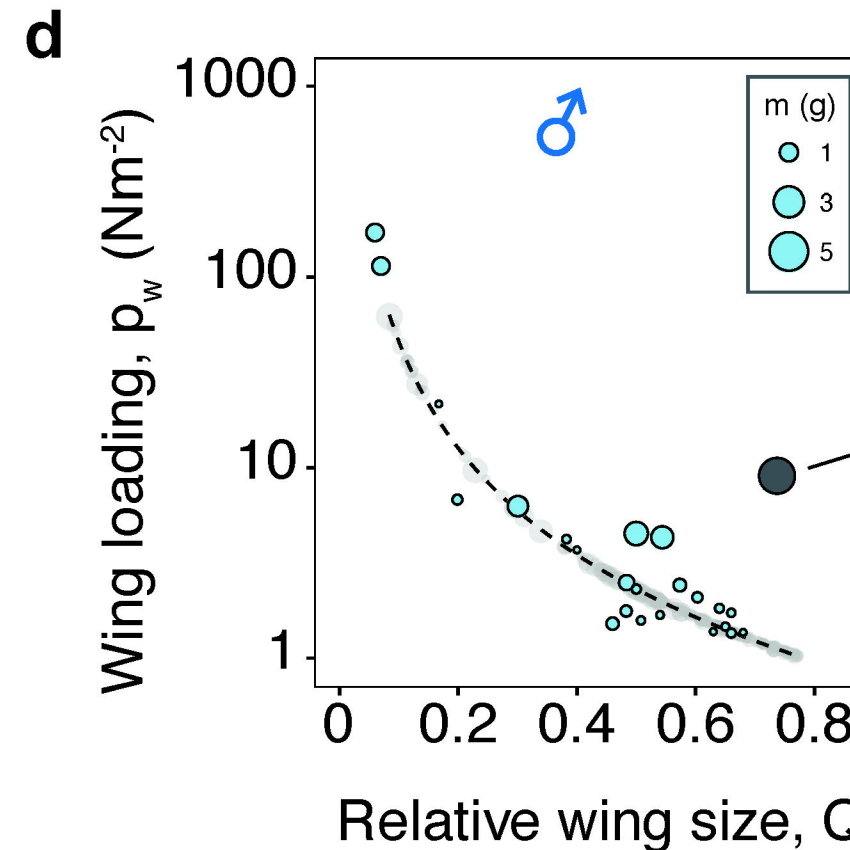
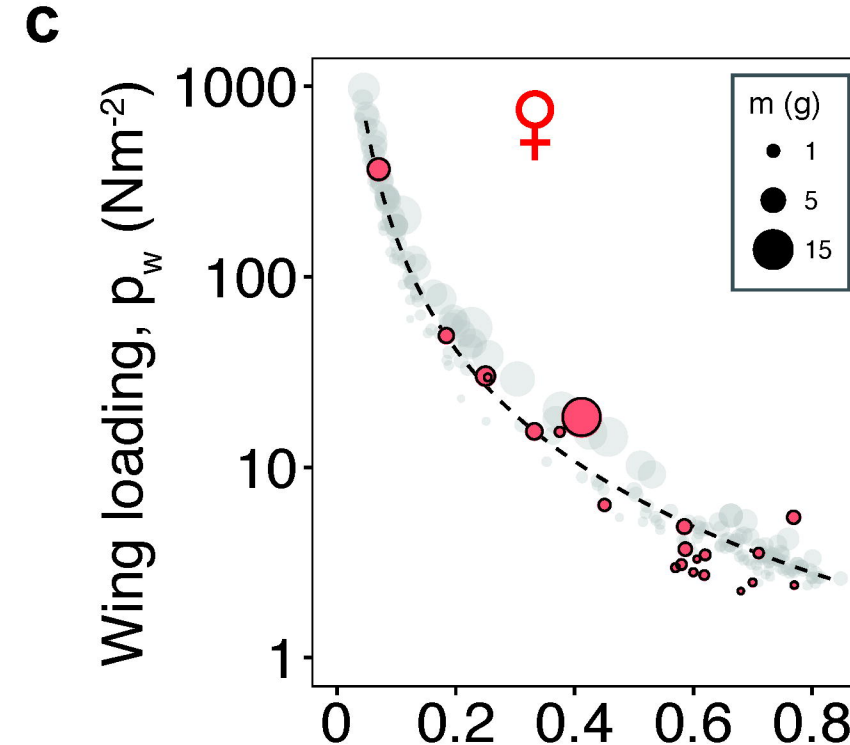
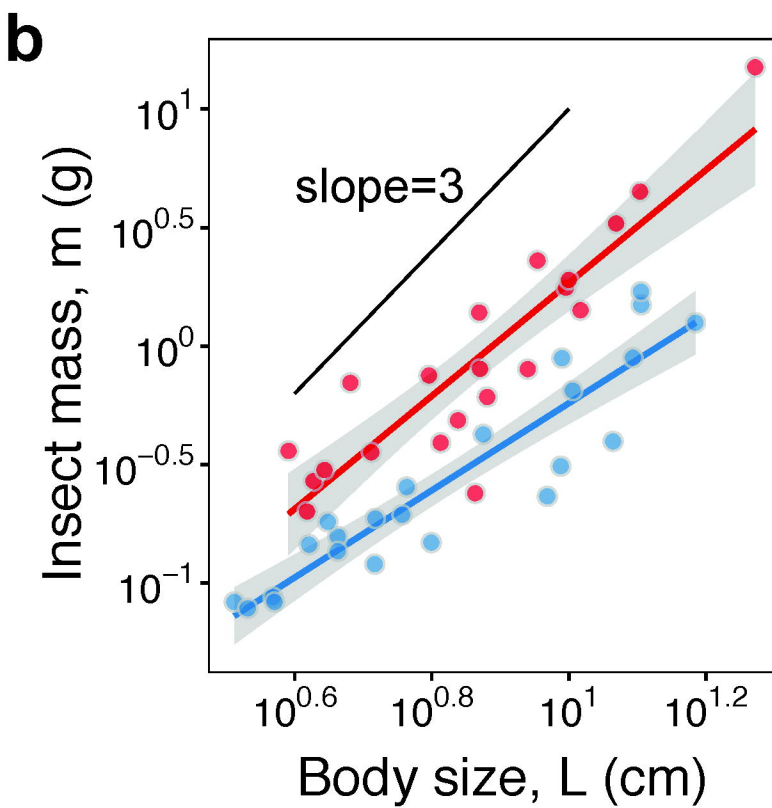
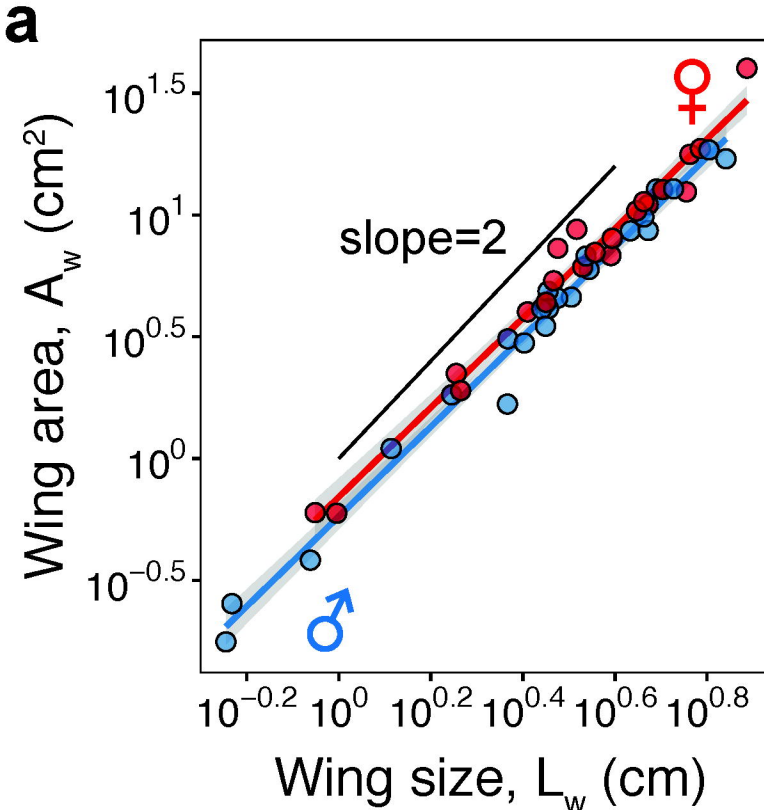
		PGLS				
		correlations	N	slope	slope.SE	P
Short-wing species	Male	$Q_M \sim \text{Log}_{10}(L_M)$	33	0.056 (0.001)	0.064 (0)	0.386 (0.011)
	Female	$Q_F \sim \text{Log}_{10}(L_F)$	88	0.015 (0.001)	0.036	0.684 (0.023)
		$Q_F \sim Q_M$	17	1.368 (0.01)	0.132 (0.003)	< 0.001
	Wing size, species-wise comparison	$Q_M \sim \Delta Q$	21	0.28 (0.001)	0.066 (0.001)	< 0.001
		$Q_F \sim \Delta Q$	21	0.018 (0.001)	0.073 (0)	0.812 (0.012)
		$\Delta Q \sim \Delta L$	21	-1.021 (0.009)	0.705 (0.003)	0.163 (0.003)
		$\Delta Q \sim L_{\text{mean}}$	21	0	0.001	0.944 (0.015)
	Body size, species-wise comparison	$L_M \sim L_F$	21	0.724 (0.001)	0.038 (0)	< 0.001
		$L_F \sim \Delta L$	21	-339.999 (2.652)	182.43 (0.708)	0.078 (0.003)
		$L_M \sim \Delta L$	21	-130.135 (2.244)	144.314 (0.636)	0.379 (0.009)
		$\Delta L \sim L_{\text{mean}}$	21	0	0	0.166 (0.005)
Long-wing species	Male	$Q_M \sim \text{Log}_{10}(L_M)$	240	-0.125 (0.005)	0.045 (0)	0.007 (0.002)
	Female	$Q_F \sim \text{Log}_{10}(L_F)$	174	-0.192 (0.004)	0.068 (0)	0.005 (0.001)
		$Q_F \sim Q_M$	114	0.654 (0.017)	0.117 (0.002)	< 0.001
	Wing size, species-wise comparison	$Q_M \sim \Delta Q$	114	0.181 (0.006)	0.082 (0.001)	0.029 (0.005)
		$Q_F \sim \Delta Q$	114	-0.964 (0.006)	0.079 (0.001)	< 0.001
		$\Delta Q \sim \Delta L$	114	-0.107 (0.02)	0.117 (0.002)	0.371 (0.097)
		$\Delta Q \sim L_{\text{mean}}$	114	0.001	0	0.023 (0.005)
	Body size, species-wise comparison	$L_M \sim L_F$	114	0.59 (0.002)	0.024 (0.001)	< 0.001
		$L_F \sim \Delta L$	114	-81.532 (4.94)	24.047 (0.817)	0.001 (0.001)
		$L_M \sim \Delta L$	114	47.087 (3.46)	17.015 (0.618)	0.008 (0.006)
		$\Delta L \sim L_{\text{mean}}$	114	-0.001 (0)	0	0.034 (0.003)

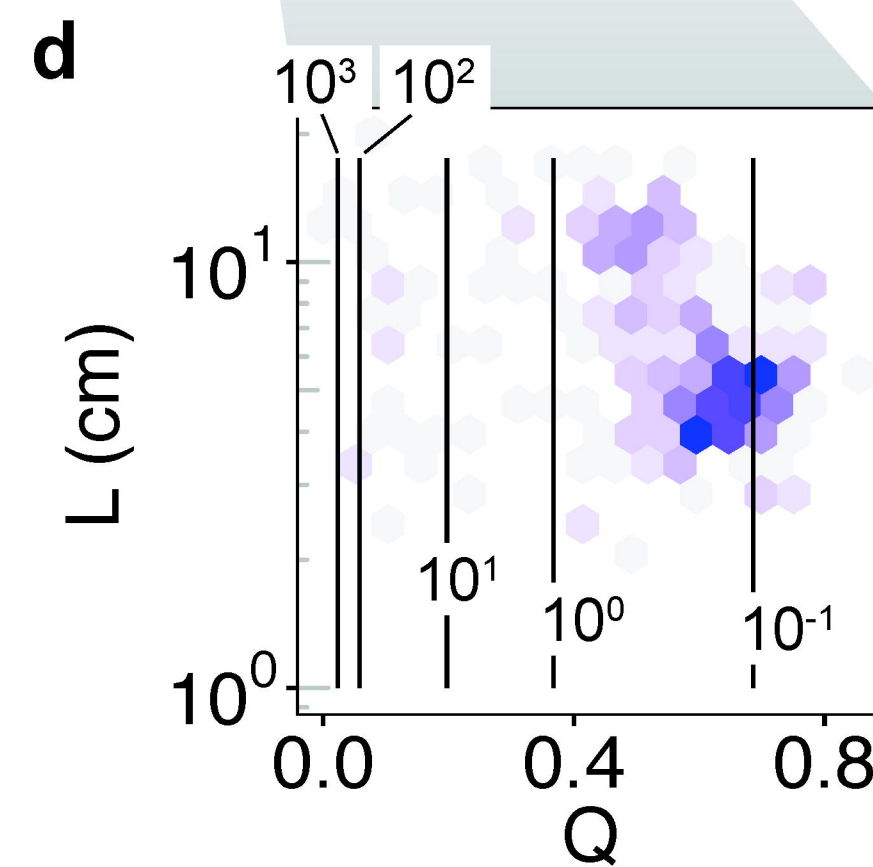
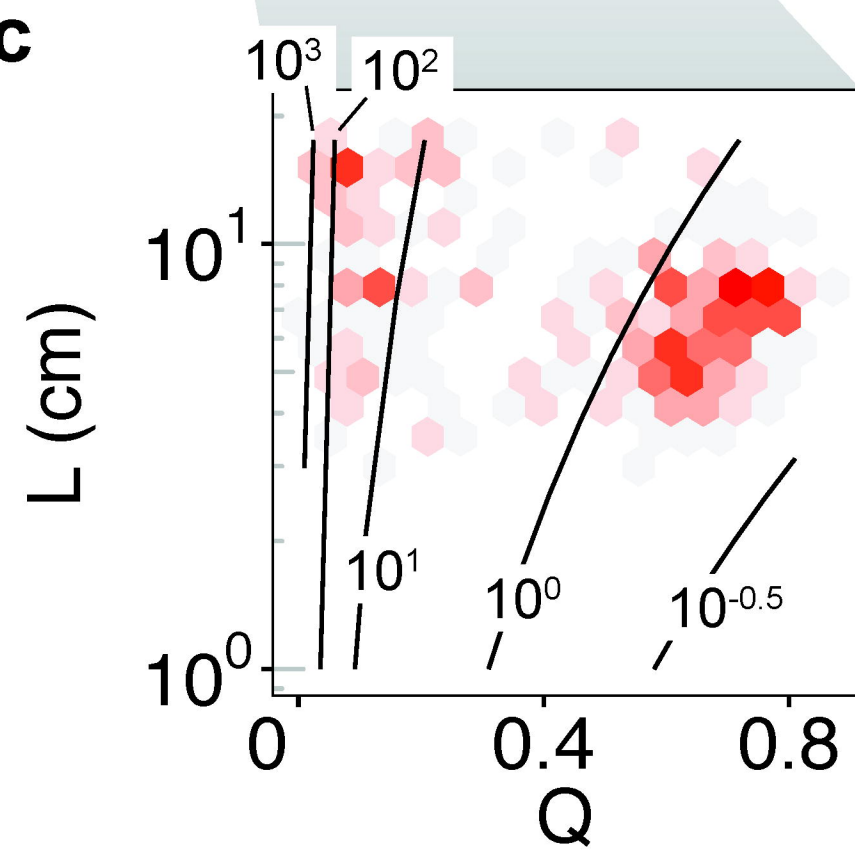
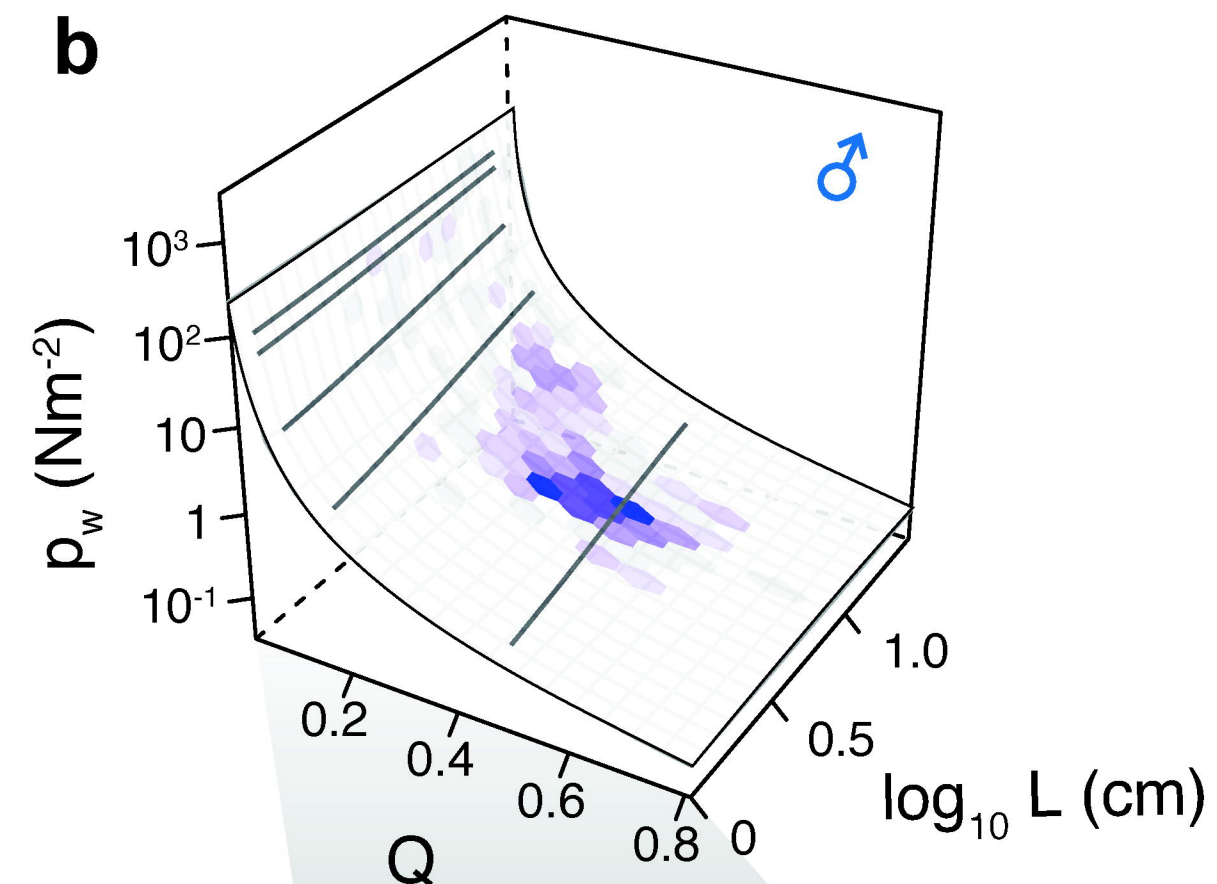
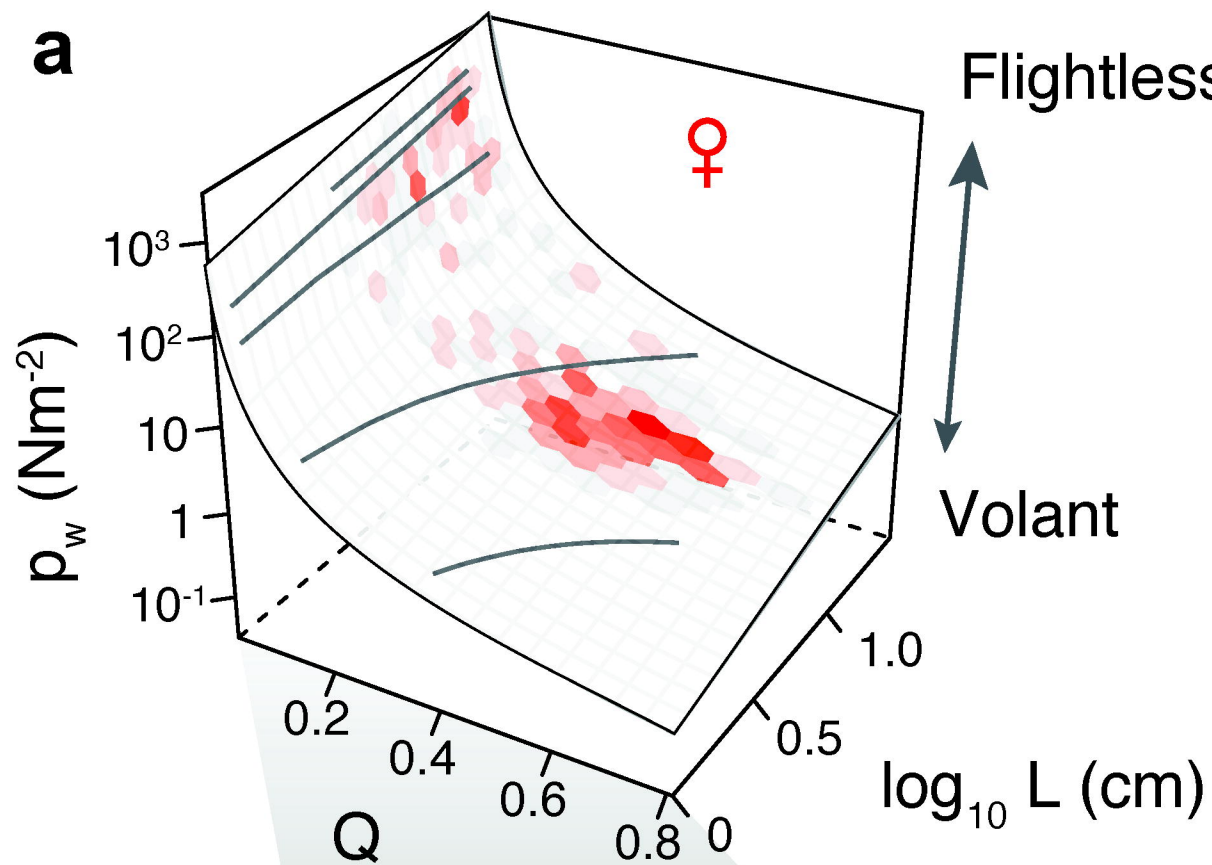
698 **Table 3.** Summary of pairwise correlational analyses using PGLS. Values represent means from
 699 analyses using 100 randomly resolved trees, with 1 s.d. in brackets.

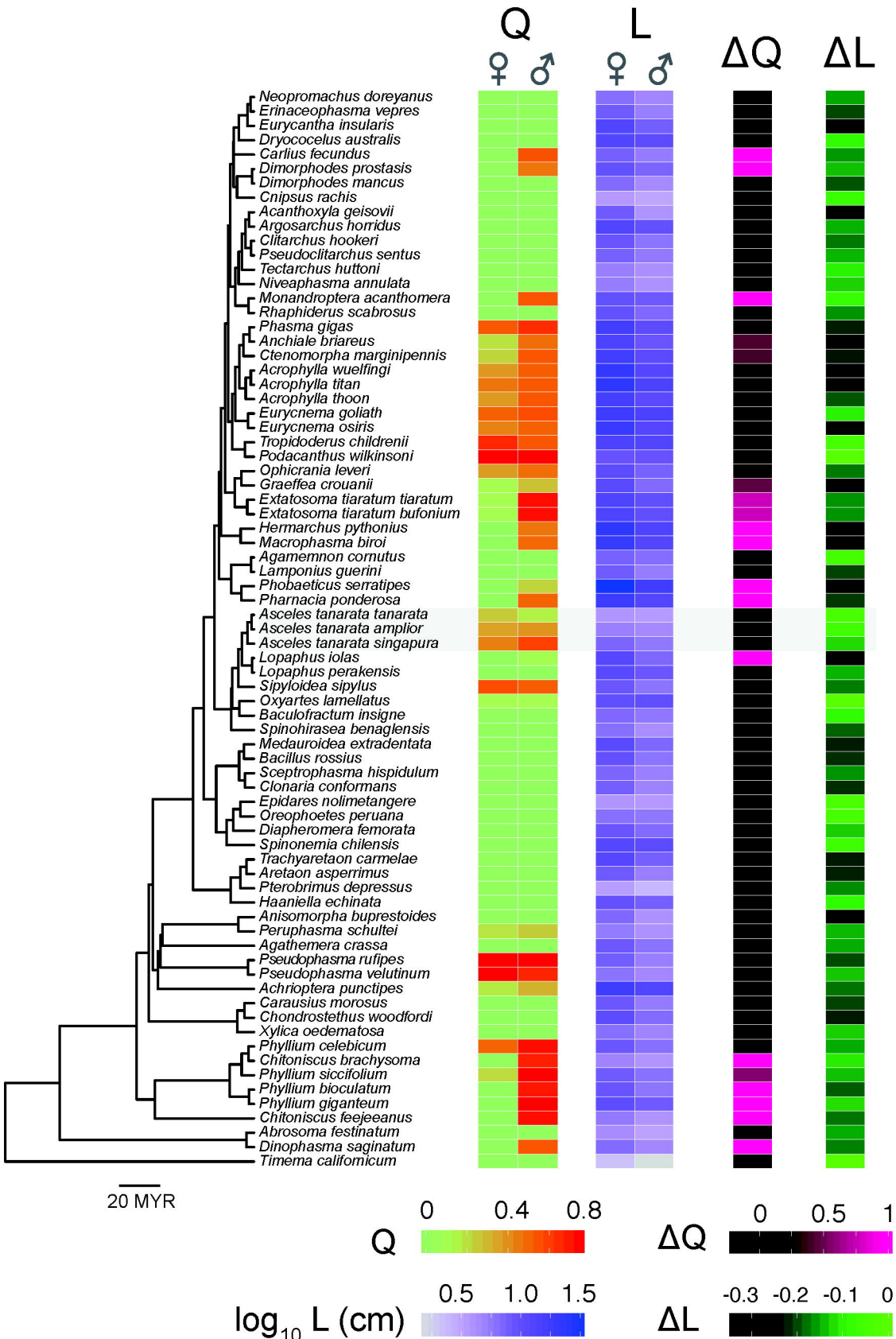
a**b**







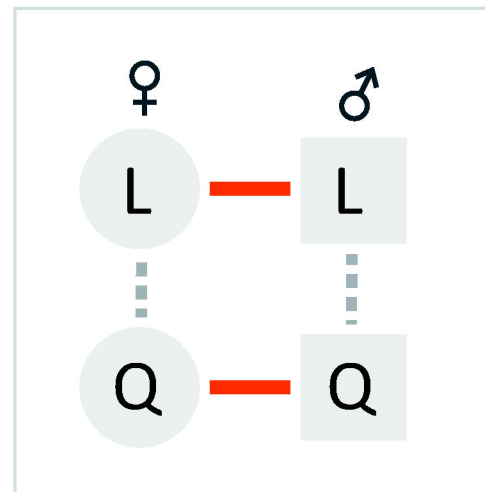




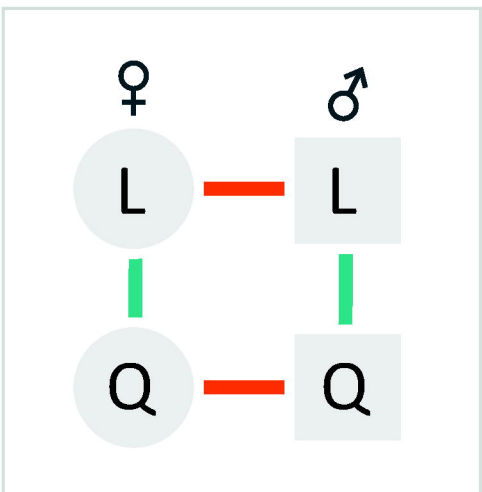
a

bioRxiv preprint first posted online Sep. 19, 2019; doi: <http://dx.doi.org/10.1101/774067>. The copyright holder for this preprint (which was not peer-reviewed) is the author/funder, who has granted bioRxiv a license to display the preprint in perpetuity. It is made available under a CC-BY-NC-ND 4.0 International license.

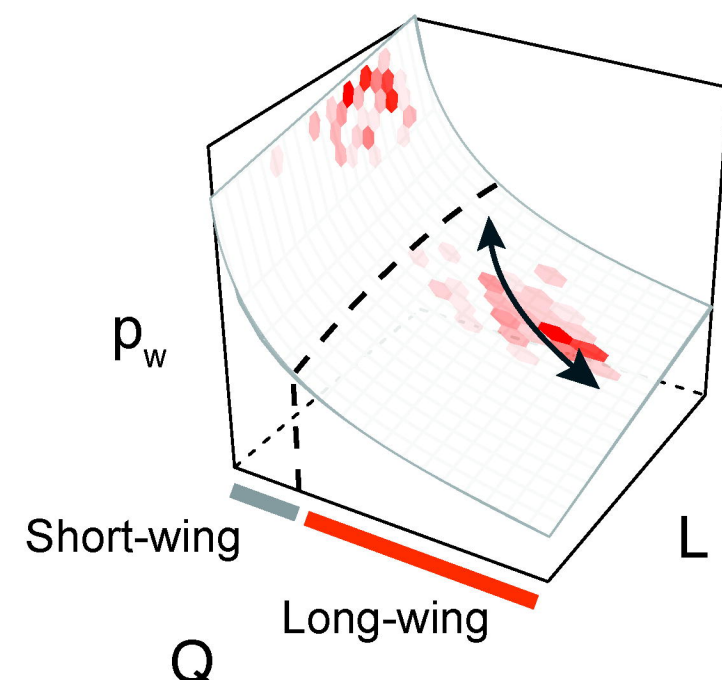
Short-wing species



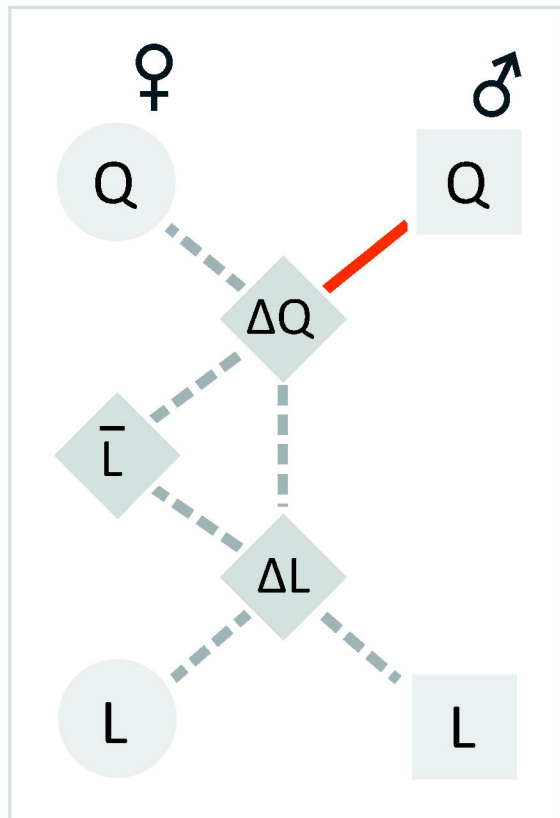
Long-wing species



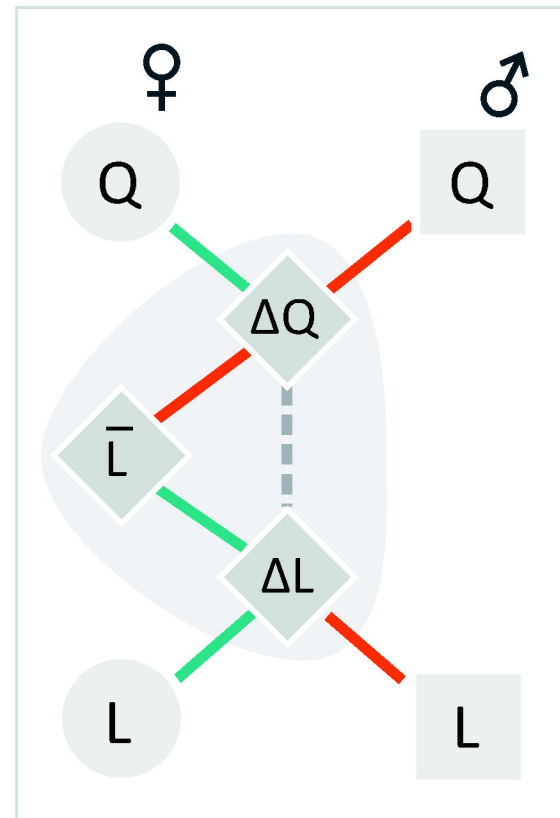
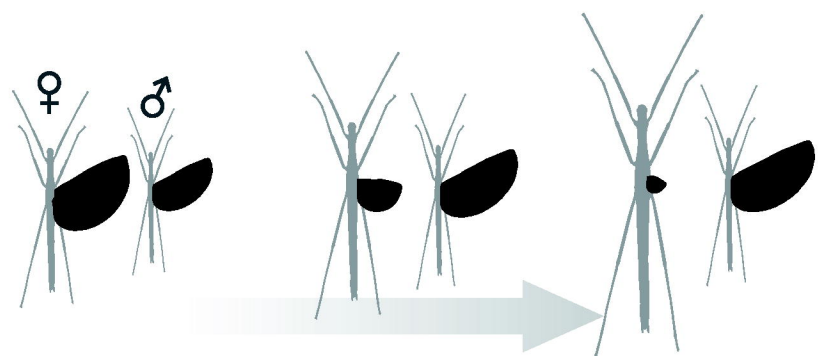
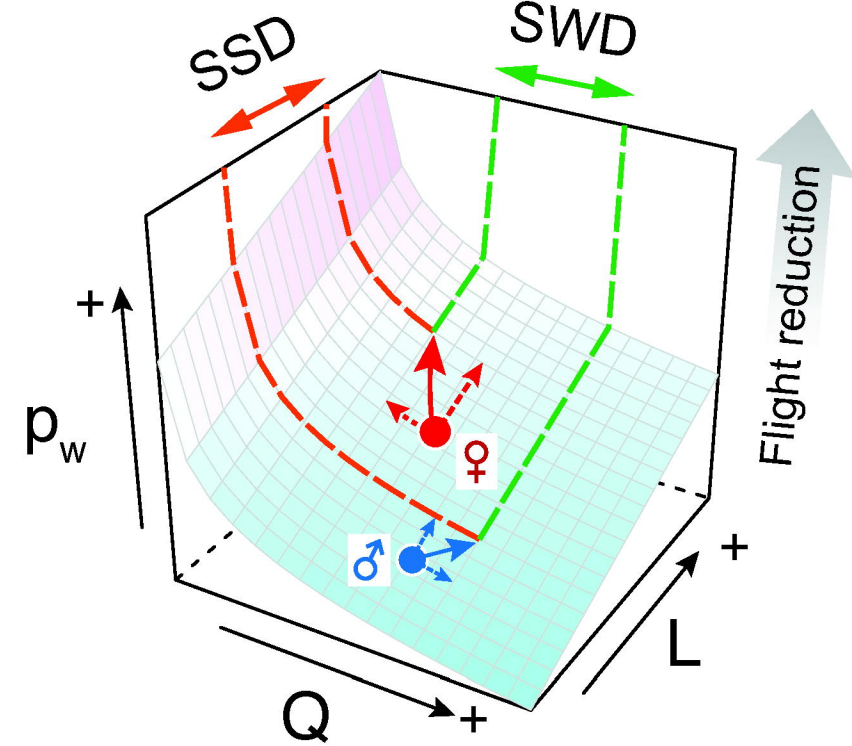
- Positive
- Negative
- Non-significant

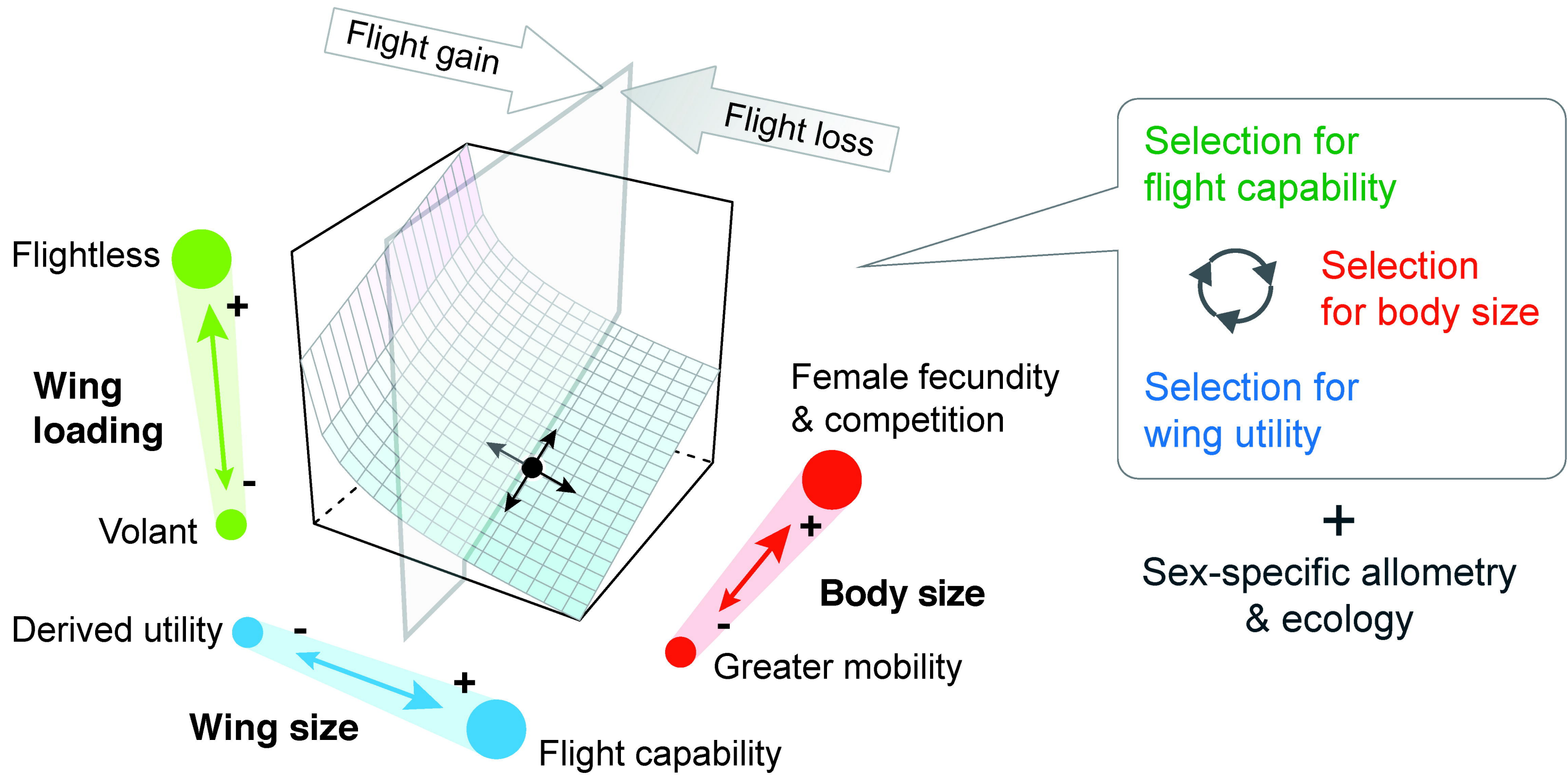
b**c**

Short-wing species



Long-wing species

**d**
 $\bar{L} \uparrow \quad \Delta L \downarrow \quad \Delta Q \uparrow$
e

a**b**